



**Development of a Hydrophilic Interaction Liquid
Chromatography (HILIC) Method for the Chemical
Characterization of Water-Soluble Isoprene Epoxydiol
(IEPOX)-Derived Secondary Organic Aerosol**

Journal:	<i>Environmental Science: Processes & Impacts</i>
Manuscript ID	EM-ART-07-2018-000308.R1
Article Type:	Paper
Date Submitted by the Author:	13-Sep-2018
Complete List of Authors:	<p>Cui, Tianqu; University of North Carolina at Chapel Hill, Environmental Sciences and Engineering Zeng, Zhexi; University of North Carolina at Chapel Hill, Department of Environmental Sciences and Engineering dos Santos, Erickson; Universidade Federal do Amazonas, Chemistry Zhang, Zhenfa; University of North Carolina at Chapel Hill, Chen, Yuzhi; University of North Carolina at Chapel Hill, Department of Environmental Sciences and Engineering Zhang, Yue; University of North Carolina at Chapel Hill, Department of Environmental Sciences and Engineering Rose, Caitlin; University of North Carolina at Chapel Hill, Department of Environmental Sciences and Engineering Budisulistiorini, Sri; University of North Carolina at Chapel Hill, Department of Environmental Sciences and Engineering Collins, Leonard; University of North Carolina at Chapel Hill, Department of Environmental Sciences and Engineering Bodnar, Wanda; University of North Carolina at Chapel Hill, Environmental Sciences and Engineering de Souza, Rodrigo; Universidade do Estado do Amazonas Martin, Scot; Harvard, SEAS Machado, Cristine; Universidade Federal do Amazonas, Chemistry Turpin, Barbara; University of North Carolina at Chapel Hill, Department of Environmental Sciences and Engineering Gold, Avram; University of North Carolina at Chapel Hill, Environmental Sciences & Engineering Ault, Andrew; University of Michigan, Environmental Health Sciences Surratt, Jason; University of North Carolina at Chapel Hill, Department of Environmental Sciences and Engineering</p>

1
2
3
4
5
6
7
8
9
10
11
12
13
14
15
16
17
18
19
20
21
22
23
24
25
26
27
28
29
30
31
32
33
34
35
36
37
38
39
40
41
42
43
44
45
46
47
48
49
50
51
52
53
54
55
56
57
58
59
60

1
2
3
4
5
6
7
8
9
10
11
12
13
14
15
16
17
18
19
20
21
22
23
24
25
26
27
28
29
30
31
32
33
34
35
36
37
38
39
40
41
42
43
44
45
46
47
48
49
50
51
52
53
54
55
56
57
58
59
60

1 **Development of a Hydrophilic Interaction Liquid Chromatography (HILIC) Method for**
2 **the Chemical Characterization of Water-Soluble Isoprene Epoxydiol (IEPOX)-Derived**
3 **Secondary Organic Aerosol**

4 Tianqu Cui^{1,a}, Zhexi Zeng^{1,a}, Erickson O. dos Santos², Zhenfa Zhang¹, Yuzhi Chen¹, Yue
5 Zhang^{1,3}, Caitlin A. Rose¹, Sri H. Budisulistiorini^{1,b}, Leonard B. Collins¹, Wanda M. Bodnar¹,
6 Rodrigo A. F. de Souza⁴, Scot T. Martin^{5,6}, Cristine M. D. Machado², Barbara J. Turpin¹, Avram
7 Gold¹, Andrew P. Ault^{7,8}, Jason D. Surratt^{1,*}

8 ¹ Department of Environmental Sciences and Engineering, Gillings School of Global Public
9 Health, The University of North Carolina at Chapel Hill, Chapel Hill, North Carolina, USA

10 ² Department of Chemistry, Federal University of Amazonas, Manaus, Amazonas, Brazil

11 ³ Aerodyne Research Inc., Billerica, Massachusetts, USA

12 ⁴ Superior School of Technology, University of the State of Amazonas, Manaus, Amazonas,
13 Brazil

14 ⁵ School of Engineering and Applied Sciences, Harvard University, Cambridge, Massachusetts,
15 USA

16 ⁶ Department of Earth and Planetary Sciences, Harvard University, Cambridge, Massachusetts,
17 USA

18 ⁷ Department of Environmental Health Sciences, University of Michigan, Ann Arbor, Michigan,
19 USA

20 ⁸ Department of Chemistry, University of Michigan, Ann Arbor, Michigan, USA

21
22 ^a These authors contributed equally to the work presented here.

23 ^b Current address: Earth Observatory of Singapore, Nanyang Technological University,
24 Singapore

25
26
27 *To whom correspondence should be addressed.

28 Tel: (919)-966-0470. Fax: (919)-966-7911. Email: surratt@unc.edu (J.D.S.)

29
30
31 The authors declare no conflict of interest.
32
33
34
35

1
2
3
4
5
6
7
8
9
10
11
12
13
14
15
16
17
18
19
20
21
22
23
24
25
26
27
28
29
30
31
32
33
34
35
36
37
38
39
40
41
42
43
44
45
46
47
48
49
50
51
52
53
54
55
56
57
58
59
60

36 For Submission to: Environmental Science: Processes & Impacts
37

Abstract

Acid-catalyzed multiphase chemistry of isoprene epoxydiols (IEPOX) on sulfate aerosol produces substantial amounts of water-soluble secondary organic aerosol (SOA) constituents, including 2-methyltetrols, methyltetrol sulfates, and oligomers thereof in atmospheric fine particulate matter (PM_{2.5}). These constituents have commonly been measured by gas chromatography interfaced to electron ionization mass spectrometry (GC/EI-MS) with prior derivatization or by reverse-phase liquid chromatography interfaced to electrospray ionization high-resolution mass spectrometry (RPLC/ESI-HR-MS). However, both techniques have limitations in explicitly resolving and quantifying polar SOA constituents due either to thermal degradation or poor separation. With authentic 2-methyltetrol and methyltetrol sulfate standards synthesized in-house, we developed a hydrophilic interaction liquid chromatography (HILIC)/ESI-HR-quadrupole time-of-flight mass spectrometry (QTOFMS) protocol that can chromatographically resolve and accurately measure the major IEPOX-derived SOA constituents in both laboratory-generated SOA and atmospheric PM_{2.5}. 2-Methyltetrols were simultaneously resolved along with 4-6 diastereomers of methyltetrol sulfate, allowing efficient quantification of both major classes of SOA constituents by a single non-thermal analytical method. The sum of 2-methyltetrols and methyltetrol sulfates accounted for approximately 92%, 62%, and 21% of the laboratory-generated β -IEPOX aerosol mass, laboratory-generated δ -IEPOX aerosol mass, and organic aerosol mass in the southeastern U.S., respectively, where the mass concentration of methyltetrol sulfates were 171-271% the mass concentration of methyltetrol. Mass concentrations of methyltetrol sulfates were 0.39 and 2.33 $\mu\text{g m}^{-3}$ in a PM_{2.5} sample collected from central Amazonia and the southeastern U.S., respectively. The improved resolution clearly reveals isomeric patterns specific to methyltetrol sulfates from acid-catalyzed multiphase

1
2
3 61 chemistry of β - and δ -IEPOX. We also demonstrate that conventional GC/EI-MS analyses
4
5 62 overestimate 2-methyltetrols by up to 188%, resulting (in part) from the thermal degradation of
6
7 63 methyltetrol sulfates. Lastly, C_5 -alkene triols and 3-methyltetrahydrofuran-3,4-diols are found to
8
9 64 be largely GC/EI-MS artifacts formed from thermal degradation of 2-methyltetrol sulfates and 3-
10
11 65 methyltetrol sulfates, respectively, and are not detected with HILIC/ESI-HR-QTOFMS.
12
13

14 66 **Environmental Significance**

15
16
17 67 $PM_{2.5}$ adversely affects air quality and human health. Isoprene is the most abundant non-
18
19 68 methane volatile organic compound primarily emitted from biogenic sources to Earth's
20
21 69 atmosphere. Atmospheric oxidation of isoprene yields large quantities of gaseous IEPOX by
22
23 70 hydroxyl radicals under low-nitric oxide conditions. IEPOX subsequently undergoes acid-
24
25 71 catalyzed multiphase chemistry with natural or anthropogenic sulfate aerosol, producing
26
27 72 substantial amounts of water-soluble IEPOX-derived SOA in $PM_{2.5}$. The HILIC/ESI-HR-
28
29 73 QTOFMS method presented here overcomes limitations of commonly utilized analytical
30
31 74 techniques, making it possible to identify and quantify water-soluble SOA constituents by a
32
33 75 single analytical method. Atmospheric chemistry model predictions of the water-soluble IEPOX-
34
35 76 derived SOA constituents (e.g., 2-methyltetrols and methyltetrol sulfates) in $PM_{2.5}$ can now be
36
37 77 assessed with greater accuracy and confidence.
38
39
40
41

42 78 **1. Introduction**

43
44 79 Atmospheric fine particulate matter ($PM_{2.5}$, aerosol particles with aerodynamic diameters
45
46 80 $\leq 2.5 \mu\text{m}$) adversely affects air quality. High concentrations of $PM_{2.5}$ can lead to degradation of
47
48 81 outdoor visibility¹ and adversely affect human health through cardiovascular and respiratory
49
50 82 diseases.² Moreover, atmospheric $PM_{2.5}$ plays a critical role in climate change through both direct
51
52 83 and indirect mechanisms.³ Organic aerosol (OA) constituents are recognized to contribute a
53
54
55
56
57
58
59
60

1
2
3 84 substantial fraction of PM_{2.5} mass from urban to remote regions around the world.⁴ OA is further
4
5 85 characterized into primary organic aerosol (POA) and secondary organic aerosol (SOA). POA is
6
7 86 directly emitted in the particle phase from sources, such as sea spray, wildfires, automobiles and
8
9
10 87 cooking, while SOA is formed from the atmospheric oxidation of volatile organic compounds
11
12 88 (VOCs) emitted by both anthropogenic and natural sources. Specifically, low volatile oxidation
13
14 89 products from VOCs either nucleate or condense onto existing particles and undergo multiphase
15
16
17 90 chemistry to form SOA, which is estimated to contribute 70-90% of OA mass found within
18
19 91 PM_{2.5}.⁵

20
21
22 92 Isoprene is the most abundant non-methane hydrocarbon emitted into Earth's atmosphere
23
24 93 and is derived largely from deciduous trees.⁶ The atmospheric oxidation of isoprene plays an
25
26 94 important role in both tropospheric ozone (O₃) and SOA formation in forested regions affected
27
28 95 by anthropogenic activities.⁷⁻¹⁴ The hydroxyl radical (OH)-initiated oxidation of isoprene during
29
30
31 96 the daytime under low-nitric oxide (NO) conditions produces substantial amounts of isoprene
32
33 97 epoxydiols (IEPOX) (~50% yield).^{15,16} The acid-catalyzed multiphase chemistry (reactive uptake)
34
35 98 of IEPOX onto anthropogenic sulfate particles have been shown to produce SOA constituents
36
37 99 including 2-methyltetrols,^{8,9,17,18} C₅-alkene triols,^{8,9,17,18} 3-methyltetrahydrofuran-3,4-diols (3-
38
39 MeTHF-3,4-diols),⁹ organosulfates,^{9,18,19,20} and oligomers.^{9,18,21} Studies have also pointed out
40 100 that the mixed effects of sulfate (e.g., aerosol acidity, nucleophile, surface area, and salting-in)
41
42 101 play a critical role in forming atmospheric IEPOX-derived SOA.^{10,19,22-24}

43
44 102
45
46
47 103 Protocols for chemical characterization of IEPOX-derived SOA C₅ tracers, including the
48
49 104 2-methyltetrols, C₅-alkene triols, and 3-MeTHF-3,4-diols, have generally employed gas
50
51 105 chromatography interfaced to electron ionization mass spectrometry (GC/EI-MS) with prior
52
53 106 trimethylsilylation.^{8,9,17-19,25} These tracer species have been widely used to investigate SOA

1
2
3 107 formation mechanisms, derive kinetic parameters, and evaluate model performance of IEPOX-
4
5 108 derived SOA.^{9,17,26,27} However, volatility and composition analysis by a Filter Inlet for Gases and
6
7
8 109 Aerosol coupled to a Chemical Ionization Mass Spectrometer (FIGAERO-CIMS) equipped with
9
10 110 iodide reagent ion chemistry demonstrated that IEPOX-derived SOA has lower volatility than
11
12 111 predicted from the concentrations of commonly reported IEPOX SOA C₅ tracers, in particular
13
14 112 the 2-methyltetrols, C₅-alkene triols and 3-MeTHF-3,4-diols, and therefore thermal
15
16
17 113 decomposition of accretion products (oligomers) or other low volatile organics such as
18
19 114 organosulfates may contribute significantly to tracers.²⁸ A second set of studies using
20
21 115 FIGAERO-CIMS or semi-volatile thermal desorption aerosol gas chromatogram (SV-TAG)
22
23 116 instrumentation with online derivatization reached similar conclusions on the impact of thermal
24
25
26 117 decomposition.²⁹⁻³² Different protocols, based on ultra-performance liquid chromatography
27
28 118 interfaced to high-resolution tandem mass spectrometry with electrospray ionization (UPLC/ESI-
29
30 119 HR-MSⁿ), have been used to characterize organosulfates and oligomers. However, separation of
31
32
33 120 polar, water-soluble components is conventionally attempted with reverse-phase liquid
34
35 121 chromatography (RPLC) columns.^{8,9,19,33} RPLC columns do not resolve such compounds well
36
37 122 because of either extremely short retention times (RTs), poor peak shapes, or ion suppression
38
39 123 effects due to co-eluting inorganic aerosol constituents, leading to potential complications in
40
41 124 identifying and quantifying target compounds. The IEPOX-derived polyols are hydrophilic
42
43
44 125 compounds owing to their hydroxyl functional groups, and the organosulfates are ionic polar
45
46 126 compounds.^{28,33} Hence, an alternative approach for the IEPOX-derived SOA characterization
47
48 127 that could accomplish simultaneous analysis of polar and water-soluble components while
49
50 128 avoiding the drawbacks associated with current analytical methods would be highly desirable.
51
52
53
54
55
56
57
58
59
60

1
2
3 129 Hydrophilic interaction liquid chromatography (HILIC) is as an alternative LC method to
4
5 130 RPLC to separate hydrophilic (i.e., water-soluble) compounds, including peptides and nucleic
6
7 131 acids³⁴ and has recently been reported to separate water-soluble organosulfates with excellent
8
9 132 resolution.³⁵⁻³⁷ The HILIC solid phase can be silica gel with a decreased surface concentration of
10
11 133 silanol groups, or silica chemically bonded to polar groups, such as amino, amide, cyano,
12
13 134 carbamate, diol, polyol, or zwitterionic sulfobetaine groups.³⁸ A HILIC column separates
14
15 135 analytes by forming a water-rich layer, which is partially immobilized around the hydrophilic
16
17 136 ligands on the stationary phase. Analytes can undergo partitioning between the bulk organic
18
19 137 eluents and the water-rich layer to separate based on different levels of retention.³⁹ Although
20
21 138 retention order on HILIC columns is similar to that on normal phase liquid chromatography
22
23 139 (NPLC) columns, HILIC utilizes more polar mobile phases (e.g., acetonitrile (ACN) and Milli-Q
24
25 140 water) than the NPLC so that the HILIC method is compatible for interfacing with ESI-MS
26
27 141 sources.⁴⁰ ESI is a soft ionization detection method not involving sample heating or
28
29 142 derivatization and is appropriate for detection of polar C₅ tracers, and oligomers as well as water-
30
31 143 soluble organosulfates. Based on the demonstrated success of HILIC in the chemical
32
33 144 characterization of organosulfates from synthesized standards and field samples,³⁵⁻³⁷ we
34
35 145 undertook development of a HILIC/ESI-HR-quadrupole time-of-flight mass spectrometry
36
37 146 (HILIC/ESI-HR-QTOFMS) method for the simultaneous separation, characterization, and
38
39 147 quantitation of water-soluble IEPOX-derived SOA constituents from laboratory-generated β -
40
41 148 IEPOX and δ -IEPOX SOA as well as PM_{2.5} collected from the southeastern U.S. at Look Rock,
42
43 149 Tennessee (TN), during Southern Oxidant and Aerosol Study (SOAS) in 2013 and central
44
45 150 Amazonia at Manaus, Brazil in 2016. The HILIC/ESI-HR-QTOFMS protocol developed here
46
47 151 can resolve IEPOX-derived 2-methyltetrols, methyltetrol sulfates and oligomers thereof,
48
49
50
51
52
53
54
55
56
57
58
59
60

1
2
3 152 allowing unambiguous identification and quantification. Current atmospheric models explicitly
4
5 153 simulate SOA from the acid-catalyzed multiphase chemistry of IEPOX (i.e., the formation of 2-
6
7 154 methyltetrols and methyltetrol sulfates),^{27,41-43} and the accurate quantification of the 2-
8
9 155 methyltetrols and the derived organosulfates will increase confidence in evaluation of model
10
11 156 predictions, which will in turn lead to improved modeling. Improvement in quantification of
12
13 157 organosulfates will additionally provide much needed data for establishing carbon and sulfur
14
15 158 mass closure in IEPOX-derived SOA measured or predicted during future lab and field studies.

19 159 **2. Experiment Section**

21 160 **2.1 Synthesized Chemicals**

23 161 **2.1.1. *Trans*- β - and δ -IEPOX**

25 162 Racemic *trans*- β -IEPOX (trans-2-methyl-2,3-epoxybutane-1,4-diol) and δ -IEPOX (3-
26
27 163 methyl-3,4-epoxy-1,2-butanediol) were synthesized in-house according to published
28
29 164 methods.^{44,45}

33 165 **2.1.2. IEPOX-Derived SOA Standards: 2-methyltetrols, 2-methyltetrol sulfates, and 3- 34 35 166 methyltetrol sulfates**

36
37 167 Diastereomeric mixtures of racemic 2-methyltetrols (racemic 2-methylerythritol and 2-
38
39 168 methylthreitol, molecular weight (MW) = 136 g mol⁻¹) were synthesized by acid hydrolysis of δ -
40
41 169 IEPOX according to the procedure described in Bondy et al.⁴⁴ A diastereomeric mixture of
42
43 170 racemic 2-methyltetrol sulfates ((2*R*,3*S*)/((2*S*,3*R*)- and (2*S*,3*S*)/(2*R*,3*R*)-1,3,4-trihydroxy-2-
44
45 171 methylbutan-2-yl sulfates, MW = 216 g mol⁻¹; Table 1) was synthesized from 2-methyltetrol.
46
47 172 Briefly, the primary and secondary hydroxyl groups of 2-methyltetrol were protected by
48
49 173 acetylation with acetic anhydride. The acetylated product was purified by column
50
51 174 chromatography on SiO₂, eluted with ethyl acetate and then sulfated by a published procedure.⁴⁶

1
2
3 175 The protecting acetyl groups were then removed by treatment with ammonia to afford the
4
5 176 expected diastereomeric 2-methyltetrol sulfates. The purity of the 2-methyltetrol sulfates was
6
7 177 determined by proton nuclear magnetic resonance (^1H NMR) spectroscopy analysis to be > 99 %
8
9 178 (Figure S1, in electronic supplementary information (SI)). The diastereomeric 3-methyltetrol
10
11 179 sulfate racemates ((*2R,3S*)/(*2S,3R*)- and (*2S,3S*)/(*2R,3R*)-2,3,4-trihydroxy-3-methylbutyl sulfates;
12
13 180 MW = 216 g mol⁻¹; Table 1) were prepared from δ -IEPOX by a procedure described in Bondy et
14
15 181 al.⁴⁴ Briefly, to an ice-cold solution of δ -IEPOX in ACN, Bu₄NHSO₄ and a small amount of
16
17 182 potassium bisulfate were added and the reaction allowed to warm to room temperature and
18
19 183 stirred overnight. The resulting mixture of sulfate esters was purified on a Dowex 50W x 4-100
20
21 184 ion exchange column. The final product contained 95.5% 3-methyltetrol sulfates by ^1H NMR
22
23 185 analysis.

29 186 **2.2 HILIC/ESI-HR-QTOFMS Method**

30
31 187 An Agilent 6520 Series Accurate Mass Q-TOFMS instrument interfaced to an Agilent
32
33 188 6500 Series UPLC system, equipped with an ESI source operated in the negative (-) ion mode,
34
35 189 was used to chemically characterize IEPOX-derived SOA standards, as well as lab and field
36
37 190 samples. Optimum ESI conditions were: 3500 V capillary voltage, 130 V fragmentor voltage, 65
38
39 191 V skimmer voltage, 300 °C gas temperature, 10 L min⁻¹ drying gas flow rate, 35 psig nebulizer,
40
41 192 25 psig reference nebulizer. ESI-QTOFMS mass spectra were recorded from mass-to-charge
42
43 193 ratio (m/z) 60 to 1000. HILIC separations were carried out using a Waters ACQUITY UPLC
44
45 194 BEH Amide column (2.1×100 mm, 1.7 μm particle size, Waters) at 35 °C. The mobile phases
46
47 195 consisted of eluent (A) 0.1% ammonium acetate in water, and eluent (B) 0.1% ammonium
48
49 196 acetate in a 95:5 (v/v) ACN (HPLC Grade, 99.9%, Fisher Scientific)/Milli-Q water. Both
50
51 197 eluents were adjusted to a pH of ~9.0 with NH₄OH.³⁵ The gradient elution program was eluent A,
52
53
54
55
56
57
58
59
60

1
2
3 198 0% for 4 min, increasing to 15% from 4 to 20 min, constant at 15% between 4 and 24 min,
4
5 199 decreasing to 0% from 24 to 25 min, and constant at 0% from 25 to 30 min. The flow rate and
6
7 200 sample injection volume were 0.3 mL min^{-1} and $5 \text{ }\mu\text{L}$, respectively. Data were acquired and
8
9 201 analyzed by Mass Hunter Version B.06.00 Build 6.0.633.0 software (Agilent Technologies). At
10
11 202 the beginning of each analysis period, the mass spectrometer was calibrated using a
12
13 203 commercially available ESI-L low-mass concentration tuning mixture (Agilent Technologies) in
14
15 204 a 95:5 (v/v) ACN/Milli-Q water. Instrument mass axis calibration was conducted in the low-
16
17 205 mass range (m/z 50-1700). Seven masses were used for calibration: m/z 68.9958, 112.9856,
18
19 206 301.9981, 601.9790, 1033.9881, 1333.9689, and 1633.9498. The adduct of hexakis (1H,1H,3H-
20
21 207 tetrafluoropropoxy) phosphazene + acetate (m/z 980.0164), purine (m/z 119.0363), and leucine
22
23 208 enkephalin (m/z 554.2620) were continuously infused for real-time mass axis correction. The
24
25 209 mass resolution of the ESI-HR-QTOFMS was approximately 8,000-12,300 from m/z 113-1600.
26
27
28
29
30

31 210 For comparison purposes, RPLC separations (Waters ACQUITY UPLC HSS T3 C₁₈
32
33 211 column, $2.1 \times 100 \text{ mm}$, $1.8 \text{ }\mu\text{m}$ particle size) were also conducted on selected samples that were
34
35 212 analyzed by HILIC, where pure methanol (99.9%, Fisher Chemical) was used as the mobile
36
37 213 phase (B) and standards and samples were prepared in 50:50 Milli-Q water/methanol. The
38
39 214 detailed operating procedures for RPLC separations have been described elsewhere.⁴⁷ In addition,
40
41 215 GC/EI-MS analysis with prior derivatization was performed following the procedures described
42
43 216 previously.^{9,18} In brief, a diluted aliquot of each filter extract was dried and trimethylsilylated by
44
45 217 reaction with $200 \text{ }\mu\text{L}$ of BSTFA + TMCS (*N,O*-bis (trimethylsilyl) trifluoroacetamide +
46
47 218 trimethylchlorosilane, 99:1, Supelco) and $100 \text{ }\mu\text{L}$ of pyridine (anhydrous, 99.8%, Sigma-
48
49 219 Aldrich). The reaction mixture was heated at $70 \text{ }^\circ\text{C}$ for 1 h and analyzed on a Hewlett-Packard
50
51 220 (HP) 5890 Series II gas chromatograph coupled to a HP 5971A mass selective detector with an
52
53
54
55
56
57
58
59
60

1
2
3 221 Econo-Cap-EC-5 capillary column (30 m × 0.25 mm i.d., 0.25 μm film thickness) within 24 h.
4
5 222 The 65-min temperature program of the GC initiated at 60 °C for 1 min, and then rose with a
6
7 223 temperature ramp of 3 °C min⁻¹ to 200 °C and isothermally held for 2 min, followed by another
8
9 224 temperature ramp of 20 °C min⁻¹ to 310 °C and isothermally held for 10 min. The temperatures of
10
11 225 both the GC inlet and detector were at 250 °C.
12
13
14

15 226 **2.3 Laboratory-Generated SOA from β- and δ-IEPOX**

16
17 227 SOA from acid-catalyzed reactive uptake of *trans*-β-IEPOX or δ-IEPOX was generated
18
19 228 in the 10-m³ indoor environmental smog chamber at the University of North Carolina as
20
21 229 described previously.^{9,23} Briefly, experiments were carried out under dark and wet conditions
22
23 230 (50-55%, RH) at 295±1 K. Prior to each experiment, the chamber was flushed continuously with
24
25 231 clean air for ~24 hours corresponding to a minimum of seven chamber volumes until the particle
26
27 232 mass concentration was < 0.01 μg m⁻³ to ensure that there were no pre-existing aerosol particles.
28
29 233 Chamber flushing also reduced VOC concentrations below the detection limit (~75 ppt for
30
31 234 IEPOX) of an iodide-adduct high-resolution time-of-flight chemical ionization mass
32
33 235 spectrometer (HR-TOF-CIMS). Operating details of the HR-TOF-CIMS have been previously
34
35 236 described.²³ Temperature and RH in the chamber were continuously monitored using a dew point
36
37 237 meter (Omega Engineering Inc.). Acidic (NH₄)₂SO₄ seed aerosol was injected into the pre-
38
39 238 humidified chamber using a custom-built atomizer with an aqueous solution of 0.06 M
40
41 239 (NH₄)₂SO₄ and 0.06 M H₂SO₄ until the desired total aerosol volume concentration (~75 μm³ cm⁻³)
42
43 240 was achieved. After seed injection, the chamber was left static for at least 30 min to ensure that
44
45 241 the seed aerosol was stable and uniformly mixed. Then, 30 mg of *trans*-β- or δ-IEPOX was
46
47 242 injected into the chamber at 2 L min⁻¹ for 10 min and then 4 L min⁻¹ for 50 min by passing high-
48
49
50
51
52
53
54
55
56
57
58
59
60

1
2
3 243 purity nitrogen gas through a heated manifold (60 °C) containing an ethyl acetate solution of one
4
5 244 of the IEPOX isomers described in section 2.1.1.
6
7

8 245 On completion of IEPOX injection, a filter sample was collected for the subsequent
9
10 246 offline analysis using HILIC (or RPLC)/ESI-HR-QTOFMS. Aerosols were collected onto a 47
11
12 247 mm Teflon filter (0.2 µm, Pall Scientific) in a stainless-steel filter holder for 30 min at a flow
13
14 248 rate of 13.2 L min⁻¹. The filter sample along with a blank filter taken from the same batch on the
15
16 249 day of the experiment were stored in a 20 mL scintillation vial at -20 °C prior to extraction and
17
18 250 analysis. In addition to the filter sampling, SOA generated from the reactive uptake of IEPOX
19
20 251 was collected using a particle-into-liquid sampler (PILS, Model 4001, Brechtel Manufacturing
21
22 252 Inc. - BMI) system at the end of each experiment. The aerosols were sampled through an organic
23
24 253 vapor denuder (Sunset Laboratory Inc.) and a 2.5-µm size-cut pre-impactor at a flow rate of
25
26 254 ~12.5 L min⁻¹. The sample air flow was then mixed adiabatically with a steam flow heated at
27
28 255 98.5-100 °C in the PILS condensation chamber to produce high supersaturation of water vapor
29
30 256 that grow particles to collectable sizes for collection onto a quartz impactor plate by inertial
31
32 257 impaction. Impacted droplets were transferred by a wash-flow at ~0.55 mL min⁻¹ through a
33
34 258 debubbler and the resulting bubble-free sample liquid was delivered through a tubing with an
35
36 259 inline filter into 2-mL poly vials held on an auto-collector (BMI) with a rotating carousel. Air
37
38 260 sampling rate and wash-flow rate were examined and recorded before and after each experiment.
39
40 261 Milli-Q water used in the wash-flow was spiked with 25 µM lithium bromide (LiBr, Sigma-
41
42 262 Aldrich, 99.5%) as an internal standard to correct for dilution caused by condensation of water
43
44 263 vapor during droplet collection. The dilution factor was typically from 1.1-1.2. The PILS vials
45
46 264 were promptly stored under dark conditions at 2 °C upon collection until analysis. Chamber
47
48 265 aerosol number distributions, which were subsequently converted to total aerosol surface area
49
50
51
52
53
54
55
56
57
58
59
60

1
2
3 266 and volume concentrations, were monitored by a scanning electrical mobility system (SEMS
4
5 267 v5.0, BMI) containing a differential mobility analyzer (DMA, BMI) coupled to a mixing
6
7
8 268 condensation particle counter (MCPC, Model 1710, BMI), in order to estimate the total aerosol
9
10 269 mass. Summary of the experimental conditions can be found in Table S1.
11
12

13 270 **2.4 Field Sample Collection of PM_{2.5}**

15 271 **2.4.1 Look Rock, Tennessee, Southeastern U.S.**

17
18 272 Quartz filter samples of PM_{2.5} were collected at a field site (Look Rock, TN, USA) during
19
20 273 the SOAS campaign in summer 2013 by a previously described procedure.¹² The filters were
21
22 274 stored in the dark in a -20 °C walk-in freezer until chemical analysis. The sample selected for re-
23
24 275 analysis was collected for three hours (16:00-19:00 local time) when one of the highest isoprene-
25
26 276 derived SOA concentrations was measured during the campaign.^{12,13}
27
28
29

30 277 **2.4.2 Manaus, Brazil, Central Amazonia**

31
32 278 PM_{2.5} samples were collected from November 28 - December 1 (transition of dry-to-wet
33
34 279 season), 2016 on pre-baked Tissuquartz Filters (Whatman, 20 cm × 25 cm) using a high-volume
35
36
37 280 PM_{2.5} sampler (ENERGÉTICA with PM_{2.5} Size Selective Inlet) located in the School of
38
39 281 Technology of the Amazonas State University in Manaus, Brazil, near a major road. The high-
40
41 282 volume PM_{2.5} sampler was located 6 m above the ground and was equipped with a cyclone
42
43 283 operated at 1.13 m³ min⁻¹. Sampler was flow calibrated and the filter holder was cleaned with the
44
45 284 filter extraction solvent (95:5 ACN/Milli-Q water for HILIC or methanol for RPLC) each day
46
47
48 285 before sampling to ensure no carryover between samples. All filters were pre-baked for 12 h at
49
50 286 550 °C and all samples were collected for 24 h. PM_{2.5} mass was determined by weighing filters
51
52 287 before and after sampling (at 21±2 °C, under < 50% RH). Filters were stored at -18 °C in the dark
53
54
55 288 until analysis. Similar to the sample selected from Look Rock, one sample (i.e., November 30,
56
57
58
59
60

289 2016) selected for re-analysis had the highest loading of PM_{2.5} and IEPOX-derived SOA tracers
290 (e.g. 2-methyltetrols and C₅-alkene triols) measured by GC/EI-MS among all samples.

291 **2.5 Sample Preparation for Offline Analyses**

292 **2.5.1 2-Methyltetrol and Methyltetrol Sulfate Standards**

293 The 2-methyltetrol, 2-methyltetrol sulfate and 3-methyltetrol sulfate standards were
294 stored at -20 °C until use. The standards were dissolved in a 2 mg mL⁻¹ Milli-Q water solution,
295 and then serially diluted immediately with 95:5 (v/v) ACN/Milli-Q water to 50, 10, 1, 0.25, 0.1,
296 0.025, and 0.01 µg mL⁻¹ standards. The diluted standards were kept at 4 °C and analyzed within
297 24 h of preparation with the laboratory and field samples described below.

298 **2.5.2 Laboratory-Generated IEPOX SOA Samples**

299 Blank and sample filters of SOA generated from *trans*-β-IEPOX and δ-IEPOX were
300 immersed in 22 mL of methanol and first extracted for 23 min by ultra-sonication, the water bath
301 replaced with cool water, and then extracted again for 22 min. This was done to ensure the water
302 bath inside the sonicator did not get too warm (from 25-30 °C, measured by a thermometer). The
303 extracts were filtered through polypropylene membrane syringe filters and the solvent was
304 evaporated under a gentle stream of nitrogen gas. Half of the dried methanol extracts were
305 reconstituted with 150 µL of 95:5 (v/v) ACN/Milli-Q water and then diluted by a factor of 100 or
306 50, respectively for the β-IEPOX- and δ-IEPOX-derived SOA samples, in order to prepare the
307 methyltetrol sulfates in the linear range of the calibration curves. The concentrations of the
308 methyltetrol sulfates in the 150 µL reconstituted solutions were not saturated and calculated later
309 to be 360-410 µg mL⁻¹, which were much lower than the solubility of the methyltetrol sulfates
310 that were determined to be at least 2500 µg mL⁻¹; specifically, maximum solubility was
311 determined by dissolving 25 mg of the methyltetrol sulfate standards in 10 mL of 95:5 (v/v)

1
2
3 312 ACN/Milli-Q water. The aqueous PILS samples collected for the laboratory-generated IEPOX
4
5 313 SOA near the end of the experiment were diluted by a factor of 20 using ACN in order to prepare
6
7 314 them in 95:5 (v/v) ACN/Milli-Q water, and promptly analyzed using the HILIC/ESI-HR-
8
9 315 QTOFMS method without any further pretreatment.
10
11
12

13 316 **2.5.3 Field Samples**

14
15 317 A 37-mm-diameter punch from the quartz filter from Look Rock along with a lab blank
16
17 318 filter were extracted as described above. Half of the Look Rock PM_{2.5} extract was reconstituted
18
19 319 with 150 μ L of 95:5 (v/v) ACN/Milli-Q water and then diluted by a factor of 20.
20
21
22

23 320 Similarly, a 47-mm diameter punch from the selected quartz filter from Manaus, Brazil,
24
25 321 as well as a lab blank filter, was extracted as described above. The residues were reconstituted in
26
27 322 1 mL methanol and a 0.3 mL aliquot was dried and reconstituted in 150 μ L of 95:5 (v/v)
28
29 323 ACN/Milli-Q water, and then diluted by a factor of 30 for analysis by HILIC/ESI-HR-QTOFMS.
30
31
32

33 324 **3. Results and Discussion**

34 35 325 **3.1 Separation of Standards: 2-Methyltetrols, 2- and 3-Methyltetrol Sulfates**

36
37 326 The synthesized standards of 2-methyltetrols, 2- and 3-methyltetrol sulfates (Section
38
39 327 2.1.2) were analyzed by both RPLC and HILIC columns coupled to the ESI-HR-QTOFMS. As
40
41 328 shown in the extracted ion chromatograms (EICs at m/z 215.023 \pm 0.01) in Figure 1, both 2- and
42
43 329 3-methyltetrol sulfate standards co-elute from the RPLC column as one peak at 1.5 min (Figure 1,
44
45 330 a1-a2). By contrast, the HILIC protocol resolved the 2-methyltetrol sulfate diastereomers at RTs
46
47 331 of 4.2 and 5.2 min. (Figure 1-b1 and S2). The unambiguous synthetic route allows assignment of
48
49 332 the diastereomers as the tertiary sulfates. Two additional trace peaks at RTs of 2.1 and 2.6 min
50
51 333 are also resolved and assigned to the secondary methyltetrol sulfate diastereomers
52
53 334 ((2*R*,3*S*)/(2*S*,3*R*)- and (2*S*,3*S*)/(2*R*,3*R*)-1,3,4-trihydroxy-3-methylbutan-2-yl sulfates) present as a
54
55
56
57
58
59
60

1
2
3 335 trace impurity (<1%). The standard derived from hydrolysis of δ -IEPOX shows the predominant
4
5 336 peaks at 8.0 and 8.3 min, assigned as the expected primary sulfate diastereomers (95.5%) (Figure
6
7 337 2-a1 and S2). A small quantity of the diastereomers at RTs of 2.1 and 2.6 min assigned to the
8
9 338 secondary sulfates (~1.2 %) is resolved, and the tertiary sulfates at 4.2 and 5.2 min are also
10
11 339 present in a small amount (~6.7%) (Figure 1-b2 and S2). These results are in line with the
12
13 340 resolution of diastereomers of methyltetrol sulfates observed in ambient aerosol by Hettiyadura
14
15 341 et al. using similar HILIC techniques; however, structural assignments in this past study were
16
17 342 tentative and not based on unambiguous synthetic routes.^{35,37} The secondary sulfate
18
19 343 diastereomers in the HILIC trace of the standard derived by hydrolysis of δ -IEPOX are
20
21 344 reasonably explained by a small yield of the less favored secondary hydrolysis product. The
22
23 345 presence of 2-methyltetrol sulfates (tertiary sulfates) is surprising and will be discussed in more
24
25 346 detail below in relation to the analysis of δ -IEPOX-derived SOA.

26
27
28
29
30
31 347 Comparison of the total ion chromatograms (TICs) acquired by RPLC and HILIC from
32
33 348 an IEPOX-derived SOA in Figure S3, along with Figure 1, unequivocally demonstrates the
34
35 349 superiority of HILIC for resolving the multiple diastereomeric components of SOA, especially
36
37 350 organosulfates derived from IEPOX.

38
39
40 351 Figure 2-a1 shows that the deprotonated 2-methyltetrol diastereomers (racemic 2-
41
42 352 methylerythritol and 2-methylthreitol) eluted at an identical RT of 4.0 min using the HILIC
43
44 353 column. By contrast, GC/EI-MS analysis with prior derivatization is able to separate the 2-
45
46 354 methyltetrol diastereomers.^{8,9,18} However, HILIC protocol is able to resolve diastereomers of 2-
47
48 355 and 3-methyltetrol sulfates not resolvable by either GC/EI-MS or RPLC. Importantly, the 2-
49
50 356 methyltetrols were simultaneously detected and resolved along with the methyltetrol sulfates. To
51
52
53 357 our knowledge, this HILIC/ESI-HR-QTOFMS method presents the first time that the major

1
2
3 358 IEPOX-derived SOA constituents, confirmed by authentic 2-methyltetrols, 2- and 3-methyltetrol
4
5 359 sulfates, have been chromatographically resolved and characterized by a single mass
6
7
8 360 spectrometric technique operated with one column and ionization mode.

9
10 361 The linear dynamic range for the 2-methyltetrols was 0.01-25 $\mu\text{g mL}^{-1}$ with a limit of
11
12 362 detection (LOD) of 7.74 $\mu\text{g L}^{-1}$ and a limit of quantification (LOQ) of 25.8 $\mu\text{g L}^{-1}$ (Table 1). The
13
14 363 linear dynamic range of 2-methyltetrol sulfates was 0.01-10 $\mu\text{g mL}^{-1}$, with an LOD of 1.72 $\mu\text{g L}^{-1}$
15
16 364 and an LOQ of 5.75 $\mu\text{g L}^{-1}$. The linear dynamic range of 3-methyltetrol sulfates was 0.01-25 μg
17
18
19 365 mL^{-1} , with an LOD of 3.83 $\mu\text{g L}^{-1}$ and an LOQ of 12.8 $\mu\text{g L}^{-1}$. Coefficients of determination (R^2)
20
21 366 values of the calibration curves ranged from 0.9994-1.0000. The linear dynamic ranges of the
22
23 367 organosulfates in this study are broader than those reported by Hettiyadura et al., which ranged
24
25
26 368 from 0.025-0.5 $\mu\text{g mL}^{-1}$.³⁵ The high R^2 and low LOQ values suggest the high performance of
27
28 369 HILIC method is the most effective procedure for quantification of organosulfates in IEPOX-
29
30
31 370 derived SOA.

32 33 371 **3.2 Identification of 2-Methyltetrols and Methyltetrol Sulfates in Laboratory-Generated** 34 35 372 **SOA and Ambient PM_{2.5} Samples**

36
37 373 Authentic 2-methyltetrol, 2- and 3-methyltetrol sulfate standards were used to identify
38
39 374 and quantify the corresponding SOA tracers. Figure 2 (a1-a5) compares the EICs at m/z 135.066,
40
41
42 375 which correspond to the deprotonated 2-methyltetrols resolved on the HILIC column, from the
43
44 376 10 $\mu\text{g mL}^{-1}$ standards of authentic 2-methyltetrols, aerosol filter extracts of laboratory-generated
45
46
47 377 SOA derived from *trans*- β -IEPOX and δ -IPEOX, PM_{2.5} samples from the Look Rock field site
48
49 378 during 2013 SOAS campaign and from Manaus, Brazil in November 2016. The chromatographic
50
51 379 peak at 4.0 min corresponding to the 2-methyltetrols were observed in all samples as the
52
53
54
55
56
57
58
59
60

1
2
3 380 predominant peak, which demonstrates that HILIC/ESI-HR-QTOFMS can unequivocally
4
5 381 identify the 2-methyltetrols in laboratory and ambient PM_{2.5} samples.
6
7

8 382 Figure 2 (b1-b5) compares the EICs at m/z 215.023 of 10 $\mu\text{g mL}^{-1}$ standards of authentic
9
10 383 2- and 3-methyltetrol sulfates, filter samples of laboratory-generated SOA derived from *trans*- β -
11
12 384 IEPOX and δ -IEPOX, PM_{2.5} samples collected from Look Rock during the 2013 SOAS
13
14 385 campaign and from Manaus, Brazil in November 2016, respectively. The predominant primary
15
16 386 sulfate diastereomers at RTs of 8.0 and 8.3 min in the 10 $\mu\text{g mL}^{-1}$ 3-methyltetrol sulfate standard
17
18 387 (Figure 2-b1, solid line) are present as abundant components of the laboratory-generated δ -
19
20 388 IEPOX SOA (Figure 2-b3) and as expected, were absent from the 10 $\mu\text{g mL}^{-1}$ standard of the 2-
21
22 389 methyltetrol sulfate (Figure 2-b1, dashed line), and the laboratory-generated *trans*- β -IEPOX
23
24 390 SOA (Figure 2-b2), confirming their origin as the acid-catalyzed multiphase chemistry of δ -
25
26 391 IEPOX. In addition, the diastereomeric peaks at RTs of 4.2 and 5.2 min were unexpectedly
27
28 392 present in Figure 2-b3 as major SOA products from δ -IEPOX. This diastereomeric pair can be
29
30 393 unequivocally assigned as the tertiary sulfates, which cannot be generated from δ -IEPOX
31
32 394 without isomerization. Hence the trace in Figure 2-b3 indicates importance of isomerization on
33
34 395 reactive uptake of δ -IEPOX.⁹ Furthermore, Figure 2-b2 shows only a single significant product
35
36 396 eluting at 5.2 min, indicating the presence of a single pair of enantiomer products. This peak is
37
38 397 therefore indicative of *trans*- β -IEPOX as the source, but surprisingly requires that substitution at
39
40 398 the tertiary carbon proceeds either with complete retention or complete inversion of optical
41
42 399 configuration. Since the expected S_N1 substitution mechanism generally results in epimerization
43
44 400 of asymmetric centers (i.e. diastereomeric products would be expected), the substitution is either
45
46 401 extremely rapid or involves an S_N2 mechanism. Such observations will be helpful in studies to
47
48
49
50
51
52
53
54
55
56
57
58
59
60

1
2
3 402 determine the origin and formation pathway of ambient methyltetrol sulfates. Full scan mass
4
5 403 spectra of selected chromatographic peaks at m/z 215.023 in Figure 2 are shown in Figure S4.
6
7

8 404 The 2- and 3-methyltetrol sulfates derived from β - and/or δ -IEPOX were present in
9
10 405 ambient $PM_{2.5}$ SOA collected at the Look Rock and Manaus field sites (Figure 2, b4-b5). The
11
12 406 two diastereomers arising uniquely from δ -IEPOX (8.0, 8.3 min), and predominant in the 3-
13
14 407 methyltetrol sulfate standard, were barely detected in the ambient aerosol samples. This
15
16 408 observation supports (*cis*- or *trans*-) β -IEPOX as the predominant ambient IEPOX isomer,
17
18 409 accounting for 97% of total ambient IEPOX,¹⁶ which corroborates results based on ESI-ion
19
20 410 mobility spectrometry (IMS)-HR-TOFMS as reported by Krechmer et al.⁴⁸ for the $PM_{2.5}$
21
22 411 collected from the Look Rock site during the 2013 SOAS campaign. Hence, the methyltetrol
23
24 412 sulfate diastereomers at 2.1, 2.6, 4.2, 5.2 min support β -IEPOX isomers as the major contributor
25
26 413 to the $PM_{2.5}$ collected at both of the Look Rock and Manaus field sites, which demonstrates the
27
28 414 advantage of HILIC/ESI-HR-QTOFMS in differentiation of isomers and apportionment of
29
30 415 reaction pathways.^{9,12,18}
31
32
33
34
35

36 416 **3.3 Quantification of 2-Methyltetrols and Methyltetrol Sulfates in Laboratory-Generated** 37 38 417 **SOA and Ambient $PM_{2.5}$ Samples** 39

40 418 Concentrations of the 2-methyltetrols and methyltetrol sulfates in the laboratory-
41
42 419 generated SOA collected by PILS and ambient $PM_{2.5}$ filters were quantified by HILIC/ESI-HR-
43
44 420 QTOFMS and are summarized in Table 2. For the 2- and 3-methyltetrol sulfates, integrated areas
45
46 421 of the 4-6 chromatographic peaks were summed to derive an overall response. As a result, the
47
48 422 response factor (defined as the ratio of peak area to concentration) of the 2-methyltetrol sulfate
49
50 423 standard was ~50% greater than that of the 3-methyltetrol sulfate standard. PILS sampling was
51
52 424 chosen for better mass closures and to avoid uncertainties due to filter sampling artifacts and
53
54
55
56
57
58
59
60

1
2
3 425 additional pretreatment procedures. Methyltetrol sulfates were quantified by an authentic 2-
4
5 426 methyltetrol sulfate standard since the two major chromatographic peaks (RTs at 4.2 and 5.2 min)
6
7
8 427 were consistently predominant in the standard and the PM_{2.5} samples, except that authentic 3-
9
10 428 methyltetrol sulfate was used as a standard to quantify methyltetrol sulfate in laboratory-
11
12 429 generated SOA from δ -IEPOX. The percentage of 2-methyltetrols and methyltetrol sulfates in
13
14 430 total aerosol mass is also shown in Table 2, calculated by dividing the mass concentration of
15
16
17 431 each compound by the total aerosol mass obtained from SEMS-MCPC, assuming a particle
18
19 432 density of 1.42 g cm⁻³ for β -IEPOX SOA or 1.55 g cm⁻³ for δ -IEPOX SOA (see SI for details).
20
21 433 The analytical uncertainty in the quantification was determined to be up to ~14.1% (SI). As
22
23 434 shown in Table 2, the concentration of the 2-methyltetrols in laboratory-generated *trans*- β -
24
25 435 IEPOX-derived SOA was 63.98 $\mu\text{g m}^{-3}$ (33.9% of total particle mass) and the concentration of
26
27 436 methyltetrol sulfates was 109.67 $\mu\text{g m}^{-3}$ (58.2% of total particle mass). In the laboratory-
28
29 437 generated SOA from δ -IEPOX, the concentration of the 2-methyltetrols 29.49 $\mu\text{g m}^{-3}$ (19.6% of
30
31 438 total aerosol mass) and methyltetrol sulfates was 62.98 $\mu\text{g m}^{-3}$ (41.9% of total aerosol mass).
32
33 439 Together, the two IEPOX-derived SOA tracers contributed 92.1 \pm 13.0% of the total aerosol mass
34
35 440 from β -IEPOX and 61.5 \pm 8.7% of the total aerosol mass from δ -IEPOX (Table 2). The
36
37 441 methyltetrol sulfates account for approximately twice the 2-methyltetrol mass. The mass
38
39 442 fractions of methyltetrol sulfates indicate conversion of a significant amount of inorganic sulfate
40
41 443 seed aerosol to organosulfates, supported by measurements using ion chromatography for the
42
43 444 PILS samples (Figure S5).
44
45
46
47
48

49 445 In addition to the monomeric methyltetrol sulfates (m/z 215.023), Figure 3 shows that the
50
51 446 HILIC column resolves multiple isomeric methyltetrol sulfate dimers (m/z 333.086) in laboratory
52
53 447 SOA generated from β - and δ -IEPOX, suggesting oligomeric products as a likely source of the
54
55
56
57
58
59
60

1
2
3 448 unaccounted for aerosol mass. RPLC did not resolve isomers of either species, since all water-
4
5 449 soluble species co-eluted at ~2 min (Figure S3).^{9,18} Additionally, small intensities of 2-
6
7 450 methyltetrol dimers ($C_{10}H_{21}O_7^-$, $m/z = 253.129$) were detected in ambient samples from Look
8
9 451 Rock and Manaus field sites. These dimers were not quantified due to the lack of authentic
10
11 452 standards.

12
13
14
15 453 In the Look Rock $PM_{2.5}$ sample with the highest IEPOX-derived SOA concentration
16
17 454 observed during the 2013 SOAS campaign,¹² the mass concentration of the 2-methyltetrol was
18
19 455 measured by HILIC/ESI-HR-QTOFMS to be $0.86 \mu\text{g m}^{-3}$, accounting for 5.6% of the total OA
20
21 456 mass, or 7.5% of the total organic carbon (OC) mass. The total OA mass concentration averaged
22
23 457 during the sampling period was determined to be $15.30 \mu\text{g m}^{-3}$ using an Aerodyne Aerosol
24
25 458 Chemical Speciation Monitor (ACSM),¹² and the total OC mass concentration from the same
26
27 459 sample was measured to be $5.04 \mu\text{gC m}^{-3}$ using a Sunset laboratory OC-elemental carbon (EC)
28
29 460 aerosol analyzer. Methyltetrol sulfates, quantified using the 2-methyltetrol sulfate standard, were
30
31 461 determined to be $2.33 \mu\text{g m}^{-3}$, accounting for 15.3% of the total OA (or 12.9% of the total OC)
32
33 462 mass, and significantly higher than $1.14 \mu\text{g m}^{-3}$ measured by RPLC/ESI-HR-QTOFMS.¹² This
34
35 463 discrepancy suggests that the RPLC/ESI-HR-QTOFMS method likely underestimates the
36
37 464 methyltetrol sulfate concentrations, possibly resulting from insufficient dilution of Look Rock
38
39 465 sample extracts (leading to concentrations beyond the linear range of the method), or appropriate
40
41 466 isomeric standards, or caused by ion suppression due to co-elution with other water-soluble
42
43 467 organic or inorganic aerosol components. The sum of the 2-methyltetrols and methyltetrol
44
45 468 sulfates quantified by the new method accounted for $20.9 \pm 2.9\%$ of the total OA mass in the Look
46
47 469 Rock sample during the 2013 SOAS campaign when high intensity of isoprene and
48
49
50
51
52
53
54
55
56
57
58
59
60

1
2
3 470 anthropogenic emissions (acidic sulfate aerosol) were observed, making IEPOX-derived SOA
4
5 471 the single largest contributor to the characterized OA constituents.¹²
6

7
8 472 For the Manaus sample, the HILIC/ESI-HR-QTOMS analysis measured 0.14 and 0.39 μg
9
10 473 m^{-3} for 2-methyltetrols and methyltetrol sulfates, respectively, accounting for 0.74% and 1.34%
11
12 474 of the total OC mass concentration ($8.12 \mu\text{gC m}^{-3}$ for this particular sample collected on
13
14 475 November 30, 2016) measured by a Sunset laboratory OC-EC aerosol analyzer. In addition,
15
16 476 elevated concentrations of levoglucosan ($0.46 \mu\text{g m}^{-3}$ by GC/EI-MS), EC ($1.18 \mu\text{gC m}^{-3}$ by a
17
18 477 Sunset OC-EC aerosol analyzer), and $\text{PM}_{2.5}$ ($46.1 \mu\text{g m}^{-3}$) were observed on this particular day,
19
20 478 and more generally during the November 28-30, 2016, sampling period due to the large influence
21
22 479 of biomass burning. In fact, average levoglucosan, OC, EC, and $\text{PM}_{2.5}$ concentrations during this
23
24 480 biomass burning intensive period were $0.41 \mu\text{g m}^{-3}$, $8.0 \mu\text{gC m}^{-3}$, $1.3 \mu\text{gC m}^{-3}$, and $43.6 \mu\text{g m}^{-3}$,
25
26 481 respectively. The elevated biomass burning likely explains why the IEPOX-derived SOA tracers
27
28 482 accounted for a lower % contribution to the total OC mass versus the southeastern U.S. sample
29
30 483 (Table 2), which the latter had little influences of biomass burning.
31
32

33 484 **3.4 Other Measurable Water-Soluble Organic Compounds in Ambient $\text{PM}_{2.5}$**

34
35
36 485 In addition to the targeted analysis for the 2-methyltetrols and methyltetrol sulfates, we
37
38 486 were able to detect several other isoprene-derived organosulfates in the ambient $\text{PM}_{2.5}$ samples.
39
40 487 Figure 4 shows the EICs of organosulfates with chemical formulas $\text{C}_4\text{H}_7\text{O}_7\text{S}^-$ (m/z 199, accurate
41
42 488 mass = 198.9912), $\text{C}_5\text{H}_9\text{O}_7\text{S}^-$ (m/z 213, accurate mass = 213.0069), and $\text{C}_5\text{H}_7\text{O}_7\text{S}^-$ (m/z 211,
43
44 489 accurate mass = 210.9912) detected in the $\text{PM}_{2.5}$ samples from Look Rock and Manaus. These
45
46 490 species have also been reported from other field and laboratory studies, including EICs obtained
47
48 491 from HILIC/ESI-MS.^{20,35-37} The ion of m/z 199 was confirmed as the sulfate ester derived from
49
50 492 another isoprene SOA tracer 2-methylglyceric acid in high- NO_x conditions.^{10,49} The structures of
51
52
53
54
55
56
57
58
59
60

1
2
3 493 the m/z 211 and 213 were tentatively proposed with EICs consistent with previous
4
5 494 observations.^{20,36,37}
6

7 495 **3.5 Discrepancy between HILIC/ESI-HR-QTOFMS and GC/EI-MS – Thermal** 8 9 **Degradation of Organosulfates**

10 496
11
12 497 Table 3 lists the concentrations of 2-methyltetrols in samples of SOA from β -IEPOX, δ -
13
14 498 IEPOX, Look Rock, and Manaus quantified in parallel by HILIC/ESI-HR-QTOFMS and GC/EI-
15
16 499 MS with prior derivatization. The concentrations of 2-methyltetrols determined by GC/EI-MS
17
18 500 were 204, 236, 160, and 288%, respectively, of that determined by HILIC/ESI-HR-QTOFMS.
19
20 501 The discrepancies are consistent with suggestions that GC/EI-MS overestimates semi-volatile
21
22 502 marker compounds because of thermal degradation of low volatile accretion products (e.g.,
23
24 503 oligomers or possibly organosulfates).²⁸ To investigate whether the overestimation in fact
25
26 504 resulted from thermal degradation or trimethylsilylation of the analytes, calibration curves of 2-
27
28 505 methyltetrol, 2- and 3-methyltetrol sulfates were generated by GC/EI-MS along with the four
29
30 506 SOA samples. As shown in Figure 5/S6/S7 (b-c), the isoprene-derived SOA tracers commonly
31
32 507 observed by GC/EI-MS, including C_5 -alkene triols, 2-methyltetrols, and 3-MeTHF-3,4-diols,
33
34 508 were detected in the pure 2- and 3-methyltetrol sulfate standards. Figure S6 (b-c) clearly
35
36 509 illustrates the formation of 2-methyltetrols in the GC/EI-MS analysis of the $50 \mu\text{g mL}^{-1}$ 2- and 3-
37
38 510 methyltetrol sulfate standards. The GC/EI-MS EIC of m/z 219 for the $50 \mu\text{g mL}^{-1}$ derivatized
39
40 511 standard of authentic 2-methyltetrol diastereomer mixture is characterized by peaks at RTs of
41
42 512 34.0 and 34.8 min. Peaks with relative intensities of ~ 0.25 and $\sim 5\%$ at the same RTs characterize
43
44 513 the EICs at m/z 219 of the pure 2- and 3-methyltetrol sulfate standards. The 2-methyltetrols from
45
46 514 degradation of the organosulfates can partially explain the large discrepancy measured between
47
48 515 the HILIC/ESI-HR-QTOFMS and GC/EI-MS methods. Other organosulfates and oligomers
49
50
51
52
53
54
55
56
57
58
59
60

1
2
3 516 present in the aerosol samples may also contribute to the discrepancy. The C₅-alkene triol tracers
4
5 517 for isoprene SOA, have been detected only by GC/EI-MS or SV-TAG methods.^{8,9,17,30,50} Lopez-
6
7 518 Hilfiker et al. have reported that the high concentrations of C₅-alkene triols measured in PM_{2.5}
8
9 519 samples analyzed by these procedures, in which samples are treated at high-temperature, are not
10
11 520 consistent with their estimated volatility, and suggest that these compounds are degradation
12
13 521 products of IEPOX-derived organosulfates and oligomers.²⁸ Based on the semi-quantitative
14
15 522 relationship established for the C₅-alkene triols produced from the 2-methyltetrol sulfate
16
17 523 standards prepared (SI), 30.0%, 42.8%, and 14.7% of the C₅-alkene triols measured by GC/EI-
18
19 524 MS could be attributed to the potential thermal degradation of the 2-methyltetrol sulfates in the
20
21 525 PM_{2.5} samples from laboratory-generated β-IEPOX SOA, Look Rock, and Manaus, respectively
22
23 526 (Table S2). Similarly, 11.1% of the 2-methyltetrols and approximately all 3-MeTHF-3,4-diols in
24
25 527 laboratory-generated δ-IEPOX SOA may be products of the thermal degradation of the 3-
26
27 528 methyltetrol sulfates (Table S3). As demonstrated above, thermal degradation of organosulfates
28
29 529 as well as low volatile accretion aerosol products (i.e., oligomers) explains a substantial fraction
30
31 530 of the isoprene-derived SOA tracers previously measured through analytical methods such as
32
33 531 GC/EI-MS or SV-TAG in which samples are treated at high temperatures.⁵¹ HILIC/ESI-HR-
34
35 532 QTOFMS avoids such treatment and is therefore preferred for accurate quantification of IEPOX-
36
37 533 derived SOA constituents.

38 534 **4. Conclusion**

39
40 535 The availability of authentic IEPOX-derived SOA standards was critical in developing
41
42 536 the HILIC/ESI-HR-QTOFMS method described here. This protocol was used to evaluate
43
44 537 IEPOX-derived SOA samples generated in laboratory studies or PM_{2.5} samples collected from
45
46 538 two isoprene-rich regions. The HILIC column can resolve the major water-soluble IEPOX-
47
48
49
50
51
52
53
54
55
56
57
58
59
60

1
2
3 539 derived SOA constituents, including the 2-methyltetrols, methyltetrol sulfates and the
4
5 540 corresponding dimers that are predicted to form in regional and global scale atmospheric
6
7 541 chemistry models.^{27,41-43,52-54} The major water-soluble IEPOX-derived SOA constituents can be
8
9 542 quantified by one method with improved accuracy. We have demonstrated the ability to
10
11 543 distinguish between different diastereomers of β - and δ -IEPOX-derived methyltetrol sulfates,
12
13 544 which allows the contribution of the IEPOX isomers to be apportioned with the availability of
14
15 545 authentic sulfate standards. Analysis by the HILIC method avoids high-temperatures required by
16
17 546 GC/EI-MS or SV-TAG methods which cause degradation of IEPOX-derived organosulfates and
18
19 547 oligomers to 2-methyltetrols, C₅-alkene triols, and 3-MeTHF-3,4-diols with consequent
20
21 548 distortion of actual product distributions.^{28,54}

22
23
24
25
26 549 By taking advantage of authentic standards and the HILIC/ESI-HR-QTOFMS method,
27
28 550 we have estimated the mass fractions of the 2-methyltetrols and the methyltetrol sulfates in
29
30 551 laboratory and ambient SOA samples. In summary, these two types of SOA constituents, likely
31
32 552 the two largest contributors, contributed 92.1±13.0%, 61.5±8.7% to total aerosol mass, and
33
34 553 20.9±2.9% to OA mass from the laboratory-generated β -IEPOX SOA, laboratory-generated δ -
35
36 554 IEPOX SOA, and Look Rock PM_{2.5}, respectively. These two SOA constituents contributed ~2.1%
37
38 555 to OC mass from Manaus PM_{2.5} sample, which was likely lower owing to the fact that biomass
39
40 556 burning was a large contributor to the OC mass during this sampling period whereas the Look
41
42 557 Rock PM_{2.5} sample had little influences of biomass burning. The methyltetrol sulfates are the
43
44 558 largest single contributor to the IEPOX SOA mass, contributing ~2-3 times of the mass of the 2-
45
46 559 methyltetrols. The predominant contributions of organosulfates (>90% of the reactive uptake of
47
48 560 β -IEPOX) reveal the significance of conversion of inorganic sulfate to organosulfate, implying
49
50 561 the critical role of inorganic sulfate as a nucleophile, and emphasize the importance of the
51
52
53
54
55
56
57
58
59
60

1
2
3 562 multiphase chemistry of IEPOX leading to SOA formation in the isoprene-rich regions. In
4
5 563 addition, oligomers derived from the methyltetrol sulfates and the 2-methyltetrols may explain
6
7
8 564 the missing fraction of the total aerosol mass.
9

10 565 Large abundances of methyltetrol sulfates in atmospheric PM_{2.5} could explain previous
11
12 566 observations of the low-volatility nature of IEPOX-derived SOA in ambient aerosol.²⁸ The
13
14 567 HILIC/ESI-HR-QTOFMS procedure described here can resolve water-soluble organic
15
16
17 568 constituents from isoprene photochemical products generated via non-IEPOX pathways. HILIC
18
19 569 separation can be interfaced to current RPLC/ESI-HR-QTOFMS procedures to develop two
20
21
22 570 dimensional LC/ESI-HR-QTOFMS, further enhancing resolution of hydrophilic organic
23
24 571 compounds in PM_{2.5}.
25
26
27
28
29
30
31
32
33
34
35
36
37
38
39
40
41
42
43
44
45
46
47
48
49
50
51
52
53
54
55
56
57
58
59
60

1
2
3 572 **Acknowledgements**
4

5
6 573 This work was funded by the National Science Foundation (NSF) under Atmospheric and
7 574 Geospace (AGS) Grant 1703535. This work was also support in part by the NSF under
8 575 Chemistry (CHE) Grant 1404644, and CAPES Foundation by Brazil Ministry of Education,
9 576 Brasilia, DF 70.040-020, Brazil. The UNC Biomarker Mass Spectrometry Facility, which
10 577 contains the HILIC/ESI-HR-QTOFMS instrument, is supported by the National Institute for
11 578 Environmental Health Sciences (NIEHS) Grant 5P20-ES10126.
12
13
14
15
16
17
18
19
20
21
22
23
24
25
26
27
28
29
30
31
32
33
34
35
36
37
38
39
40
41
42
43
44
45
46
47
48
49
50
51
52
53
54
55
56
57
58
59
60

579 **References**

- 580 1. Y. H. Wang, Z. R. Liu, J. K. Zhang, B. Hu, D. S. Ji, Y. C. Yu and Y. S. Wang, Aerosol
581 physicochemical properties and implications for visibility during an intense haze episode
582 during winter in Beijing, *Atmos. Chem. Phys.*, **2014**, 15 (6), 3205-3215.
- 583 2. C. I. Davidson, R. F. Phalen and P. A. Solomon, Airborne particulate matter and human
584 health: a review, *Aerosol Sci. Technol.*, **2005**, 39 (8), 737-749.
- 585 3. M. C. Jacobson, H. -C. Hansson, K. J. Noone and R. J. Charlson, Organic atmospheric
586 aerosols: review and state of the science, *Rev. Geophys.*, **2000**, 38 (2), 267-294.
- 587 4. J. L. Jimenez, M. R. Canagaratna, N. M. Donahue, A. S. H. Prevot, Q. Zhang, J. H. Kroll, P. F.
588 DeCarlo, J. D. Allan, H. Coe, N. L. Ng, A. C. Aiken, K. S. Docherty, I. M. Ulbrich, A. P.
589 Grieshop, A. L. Robinson, J. Duplissy, J. D. Smith, K. R. Wilson, V. A. Lanz, C. Hueglin, Y.
590 L. Sun, J. Tian, A. Laaksonen, T. Raatikainen, J. Rautiainen, P. Vaattovaara, M. Ehn, M.
591 Kulmala, J. M. Tomlinson, D. R. Collins, M. J. Cubison¹, E. J. Dunlea, J. A. Huffman, T. B.
592 Onasch, M. R. Alfarra, P. I. Williams, K. Bower, Y. Kondo, J. Schneider, F. Drewnick, S.
593 Borrmann, S. Weimer, K. Demerjian, D. Salcedo, L. Cottrell, R. Griffin, A. Takami, T.
594 Miyoshi, S. Hatakeyama, A. Shimono, J. Y. Sun, Y. M. Zhang, K. Dzepina, J. R. Kimmel, D.
595 Sueper, J. T. Jayne, S. C. Herndon, A. M. Trimborn, L. R. Williams, E. C. Wood, A. M.
596 Middlebrook, C. E. Kolb, U. Baltensperger, and D. R. Worsnop, Evolution of organic
597 aerosols in the atmosphere, *Science*, **2009**, 326 (5959), 1525-1529.
- 598 5. K. S. Docherty, E. A. Stone, I. M. Ulbrich, P. F. DeCarlo, D. C. Snyder, J. J. Schauer, R. E.
599 Peltier, R. J. Weber, S. M. Murphy, J. H. Seinfeld, B. D. Grover, D. J. Eatough, and J. L.
600 Jimenez, Apportionment of primary and secondary organic aerosols in Southern California
601 during the 2005 study of organic aerosols in Riverside (SOAR-1), *Environ. Sci. Technol.*,
602 **2008**, 42, 7655-7662.
- 603 6. A. Guenther, T. Karl, P. Harley, C. Wiedinmyer, P. I. Palmer, and C. Geron, Estimates of
604 global terrestrial isoprene emissions using MEGAN (Model of Emissions of Gases and
605 Aerosols from Nature), *Atmos. Chem. Phys.*, **2006**, 6, 3181-3210.
- 606 7. W. L. Chameides, R. W. Lindsay, J. Richardson, and C. S. Kiang, The role of biogenic
607 hydrocarbons in urban photochemical smog: Atlanta as a case study, *Science*, **1988**, 241
608 (4872), 1473-1475.
- 609 8. J. D. Surratt, S. M. Murphy, J. H. Kroll, N. L. Ng, L. Hildebrandt, A. Sorooshian, R.
610 Szmigielski, R. Vermeylen, W. Maenhaut, M. Claeys, R. C. Flagan, and J. H. Seinfeld,
611 Chemical composition of secondary organic aerosol formed from the photooxidation of
612 isoprene, *J. Phys. Chem. A*, **2006**, 110 (31), 9665-9690.
- 613 9. Y. -H. Lin, Z. Zhang, K. S. Docherty, H. Zhang, S. H. Budisulistiorini, C. L. Rubitschun, S. L.
614 Shaw, E. M. Knipping, E. S. Edgerton, T. E. Kleindienst, A. Gold, and J. D. Surratt, Isoprene
615 epoxydiols as precursors to secondary organic aerosol formation: acid-catalyzed reactive
616 uptake studies with authentic compounds, *Environ. Sci. Technol.*, **2012**, 46 (1), 200-258.
- 617 10. Y. -H. Lin, H. Zhang, H. O. T. Pye, Z. Zhang, W. J. Marth, S. Park, M. Arashiro, T. Cui, S.
618 H. Budisulistiorini, K. G. Sexton, W. Vizuete, Y. Xie, D. J. Luecken, I. R. Piletic, E. O.
619 Edney, L. J. Bartolotti, A. Gold, and J. D. Surratt, Epoxide as a precursor to secondary
620 organic aerosol formation from isoprene photooxidation in the presence of nitrogen oxides,
621 *Proc. Natl. Acad. Sci.*, **2013**, 110 (17) 6718-6723.
- 622 11. S. H. Budisulistiorini, M. R. Canagaratna, P. L. Croteau, W. J. Marth, K. Baumann, E. S.
623 Edgerton, S. L. Shaw, E. M. Knipping, D. R. Worsnop, J. T. Jayne, A. Gold, and J. D. Surratt,

- 1
2
3 624 Real-time continuous characterization of secondary organic aerosol derived from isoprene
4 625 epoxydiols in downtown Atlanta, Georgia, using the Aerodyne aerosol chemical speciation
5 626 monitor, *Environ. Sci. Technol.*, **2013**, 47 (11), 5685-5694.
- 6 627 12. S. H. Budisulistiorini, X. Li, S. T. Bairai, J. Renfro, Y. Liu, Y. J. Liu, K. A. McKinney, S. T.
7 628 Martin, V. F. McNeill, H. O. T. Pye, A. Nenes, M. E. Neff, E. A. Stone, S. Mueller, C. Knote,
8 629 S. L. Shaw, Z. Zhang, A. Gold, and J. D. Surratt, Examining the effects of anthropogenic
9 630 emissions on isoprene-derived secondary organic aerosol formation during the 2013 Southern
10 631 Oxidant and Aerosol Study (SOAS) at the Look Rock, Tennessee ground site, *Atmos. Chem.*
11 632 *Phys.*, **2015**, 15, 8871-8888.
- 12 633 13. S. H. Budisulistiorini, K. Baumann, E. S. Edgerton, S. T. Bairai, S. Mueller, S. L. Shaw, E.
13 634 M. Knipping, A. Gold, and J. D. Surratt, Seasonal characterization of submicron aerosol
14 635 chemical composition and organic aerosol sources in the southeastern United States: Atlanta,
15 636 Georgia, and Look Rock, Tennessee, *Atmos. Chem. Phys.*, **2016**, 16, 5171-5189.
- 16 637 14. W. Rattanavaraha, K. Chu, S. H. Budisulistiorini, M. Riva, Y. -H. Lin, E. S. Edgerton, K.
17 638 Baumann, S. L. Shaw, H. Guo, L. King, R. J. Weber, M. E. Neff, E. A. Stone, J. H. Offenberg,
18 639 Z. Zhang, A. Gold, and J. D. Surratt, Assessing the impact of anthropogenic pollution on
19 640 isoprene-derived secondary organic aerosol formation in PM_{2.5} collected from the
20 641 Birmingham, Alabama, ground site during the 2013 Southern Oxidant and Aerosol Study,
21 642 *Atmos. Chem. Phys.*, **2016**, 16, 4897-4914.
- 22 643 15. F. Paulot, J. D. Crouse, H. G. Kjaergaard, A. Kürten, J. M. St. Clair, J. H. Seinfeld, and P. O.
23 644 Wennberg, Unexpected Epoxide Formation in the Gas-Phase Photooxidation of Isoprene,
24 645 *Science*. **2009**, Aug 7; 325 (5941):730-3.
- 25 646 16. K. H. Bates, J. D. Crouse, J. M. St. Clair, N. B. Bennett, T. B. Nguyen, J. H. Seinfeld, B. M.
26 647 Stoltz, and P. O. Wennberg, Gas Phase Production and Loss of Isoprene Epoxydiols, *J. Phys.*
27 648 *Chem. A*, **2014**, 118 (7), 1237-1246.
- 28 649 17. W. Wang, I. Kourtchev, B. Graham, J. Cafmeyer, W. Maenhaut, and M. Claeys,
29 650 Characterization of oxygenated derivatives of isoprene related to 2-methyltetrols in
30 651 Amazonian aerosols using trimethylsilylation and gas chromatography/ion trap mass
31 652 spectrometry, *Rapid Commun. Mass Spectrom.* **2005**; 19: 1343-1351.
- 32 653 18. J. D. Surratt, A. W. H. Chan, N. C. Eddingsaas, M. Chan, C. L. Loza, A. J. Kwan, S. P.
33 654 Hersey, R. C. Flagan, P. O. Wennberg, and J. H. Seinfeld, Reactive intermediates revealed in
34 655 secondary organic aerosol formation from isoprene, *Proc. Natl. Acad. Sci.*, **2010**, 107 (15),
35 656 6640-6645.
- 36 657 19. J. D. Surratt, M. Lewandowski, J. H. Offenberg, M. Jaoui, T. E. Kleindienst, E. O. Edney,
37 658 and J. H. Seinfeld, Effect of acidity on secondary organic aerosol formation from isoprene,
38 659 *Environ. Sci. Technol.*, **2007**, 41 (15), 6640-6645.
- 39 660 20. J. D. Surratt, Y. Gomez-Gonzalez, A. W. H. Chan, R. Vermeylen, M. Shahgholi, T. E.
40 661 Kleindienst, E. O. Edney, J. H. Offenberg, M. Lewandowski, M. Jaoui, W. Maenhaut, M.
41 662 Claeys, R. C. Flagan, and J. H. Seinfeld, Organosulfate formation in biogenic secondary
42 663 organic aerosol, *J. Phys. Chem. A*, **2008**, 112, 8345-8378.
- 43 664 21. Y. -H. Lin, S. H. Budisulistiorini, K. Chu, R. A. Siejack, H. Zhang, M. Riva, Z. Zhang, A.
44 665 Gold, K. E. Kautzman, and J. D. Surratt, Light-absorbing oligomer formation in secondary
45 666 organic aerosol from reactive uptake of isoprene epoxydiols, *Environ. Sci. Technol.*, **2014**, 48
46 667 (20), 12012-12021.

- 1
2
3 668 22. C. J. Gaston, T. P. Riedel, Z. Zhang, A. Gold, J. D. Surratt, and J. A. Thornton, Reactive
4 669 uptake of an isoprene-derived epoxydiol to submicron aerosol particles, *Environ. Sci.*
5 670 *Technol.*, **2014**, 48 (19), 11178-11186.
- 6 671 23. T. P. Riedel, Y. -H. Lin, S. H. Budisulistiorini, C. J. Gaston, J. A. Thornton, Z. Zhang, W.
7 672 Vizquete, A. Gold, and J. D. Surratt, Heterogeneous reactions of isoprene-derived epoxides:
8 673 Reaction probabilities and molar secondary organic aerosol yield estimates, *Environ. Sci.*
9 674 *Technol. Lett.*, **2015**, 2 (2), 38-42.
- 10 675 24. L. Xu, H. Guo, C. M. Boyd, M. Klein, A. Bougiatioti, K. M. Cerully, J. R. Hite, G.
11 676 Isaacman-VanWertz, N. M. Kreisberg, C. Knote, K. Olson, A. Koss, A. H. Goldstein, S. V.
12 677 Hering, J. de Gouw, K. Baumann, S. -H. Lee, A. Nenes, R. J. Weber, and N. L. Ng, Effects of
13 678 anthropogenic emissions on aerosol formation from isoprene and monoterpenes in the
14 679 southeastern United States, *Proc. Natl. Acad. Sci.*, **2015**, 112 (1) 37-42.
- 15 680 25. M. Claeys, B. Graham, G. Vas, W. Wang, R. Vermeylen, V. Pashynska, J. Cafmeyer, P.
16 681 Guyon, M. O. Andreae, P. Artaxo, and W. Maenhaut, Formation of secondary organic
17 682 aerosols through photooxidation of isoprene, *Science*, **2004**, 303 (5661), 1173-1176.
- 18 683 26. T. P. Riedel, Y. -H. Lin, Z. Zhang, K. Chu, J. A. Thornton, W. Vizquete, A. Gold, and J. D.
19 684 Surratt, Constraining condensed-phase formation kinetics of secondary organic aerosol
20 685 components from isoprene epoxydiols, *Atmos. Chem. Phys.*, **2016**, 16 (3), 1245-1254.
- 21 686 27. S. H. Budisulistiorini, A. Nenes, A. G. Carlton, J. D. Surratt, V. F. McNeill, and H. O. T. Pye,
22 687 Simulating aqueous-phase isoprene-epoxydiol (IEPOX) secondary organic aerosol production
23 688 during the 2013 Southern Oxidant and Aerosol Study (SOAS), *Environ. Sci. Technol.* **2017**,
24 689 51 (9), 5026-5034.
- 25 690 28. F. D. Lopez-Hilfiker, C. Mohr, E. L. D'Ambro, A. Lutz, T. P. Riedel, C. J. Gaston, S. Iyer, Z.
26 691 Zhang, A. Gold, J. D. Surratt, B. H. Lee, T. Kurten, W.W. Hu, J. Jimenez, M. Hallquist, and J.
27 692 A. Thornton, Molecular composition and volatility of organic aerosol in the Southeastern U.S.:
28 693 implications for IEPOX derived SOA, *Environ. Sci. Technol.* **2016**, 50 (5), 2200-2209.
- 29 694 29. G. Isaacman, N. M. Kreisberg, L. D. Yee, D. R. Worton, A. W. H. Chan, J. A. Moss, S. V.
30 695 Hering, and A. H. Goldstein, Online derivatization for hourly measurements of gas- and
31 696 particle-phase semi-volatile oxygenated organic compounds by thermal desorption aerosol gas
32 697 chromatography (SV-TAG), *Atmos. Meas. Tech.*, **2014**, 7(12), 4417-4429.
- 33 698 30. G. Isaacman-VanWertz, L. D. Yee, N. M. Kreisberg, R. Wernis, J. A. Moss, S. V. Hering, S.
34 699 S. de Sa, S. T. Martin, M. L. Alexander, B. B. Palm, W. Hu, P. Campuzano-Jost, D. A. Day, J.
35 700 L. Jimenez, M. Riva, J. D. Surratt, J. Viegas, A. Manzi, E. Edgerton, K. Baumann, R. Souza,
36 701 P. Artaxo, and A. H. Goldstein, Ambient gas-particle partitioning of tracers for biogenic
37 702 oxidation, *Environ. Sci. Technol.*, **2016**, 50 (18), 9952-9962.
- 38 703 31. B. J. Williams, Y. Zhang, X. Zuo, R. E. Martinez, M. J. Walker, N. M. Kreisberg, A. H.
39 704 Goldstein, K. S. Docherty, and J. L. Jimenez, Organic and inorganic decomposition products
40 705 from the thermal desorption of atmospheric particles, *Atmos. Meas. Tech.*, **2016**, 9, 1569-1586
- 41 706 32. H. Stark, R. L. N. Yataavelli, S. L. Thompson, H. Kang, J. E. Krechmer, J. R. Kimmel, B. B.
42 707 Palm, W. Hu, P. L. Hayes, D. A. Day, P. Campuzano-Jost, M. R. Canagaratna, J. T. Jayne, D.
43 708 R. Worsnop, and J. L. Jimenez, Impact of thermal decomposition on thermal desorption
44 709 instruments: advantage of thermogram analysis for quantifying volatility distributions of
45 710 organic species, *Environ. Sci. Technol.*, **2016**, 51 (15), 8491-8500
- 46 711 33. Y. Gomez-Gonzalez, J. D. Surratt, F. Cuyckens, R. Szmigelski, R. Vermeylen, M. Jaoui, M.
47 712 Lewandowski, J. H. Offenberg, T. E. Kleindienst, E. O. Edney, F. Blockhuys, C. Van Alsenoy,
48 713 W. Maenhaut, and M. Claeys, Characterization of organosulfates from the photooxidation of

- 1
2
3 714 isoprene and unsaturated fatty acids in ambient aerosol using liquid chromatography/(-)
4 715 electrospray ionization mass spectrometry, *J. Mass Spectrom.*, **2008**, 43, 371-382.
- 5 716 34. A. J. Alpert, Hydrophilic-interaction chromatography for the separation of peptides, nucleic
6 717 acids and other polar compounds, *J. Chromatogr., A*, **1990**, 499 (19), 177-196.
- 7 718 35. A. P. S. Hettiyadura, E. A. Stone, S. Kundu, Z. Baker, E. Geddes, K. Richards, and T.
8 719 Humphry, Detection of atmospheric organosulfates using HILIC chromatography with MS
9 720 detection, *Atmos. Meas. Tech.*, **2015**, 8, 2347-2358.
- 10 721 36. G. Spolnik, P. Wach, K. J. Rudzinski, K. Skotak, W. Danikiewicz, and R. Szmigielski,
11 722 Improved UHPLC-MS/MS methods for analysis of isoprene-derived organosulfates, *Anal.*
12 723 *Chem.*, **2018**, 90 (5), 3416–3423.
- 13 724 37. A. P. S. Hettiyadura, T. Jayarathne, K. Baumann, A. H. Goldstein, J. A. de Gouw, A. Koss, F.
14 725 N. Keutsch, K. Skog, and E. A. Stone, Qualitative and quantitative analysis of atmospheric
15 726 organosulfates in Centreville, Alabama, *Atmos. Chem. Phys.*, **2017**, 17, 1343–1359.
- 16 727 38. P. Jandera, Stationary phases for hydrophilic interaction chromatography, their
17 728 characterization and implementation into multidimensional chromatography concepts, *J. Sep.*
18 729 *Sci.*, **2008**, 31 (9), 1421-1437.
- 19 730 39. P. Hemstrom and K. Irgum, Hydrophilic interaction chromatograph, *J. Sep. Sci.*, **2006**, 29
20 731 (12), 1784-1821.
- 21 732 40. Y. Guo and S. Gaiki, Retention behavior of small polar compounds on polar stationary
22 733 phases in hydrophilic interaction chromatography, *J. Chromatogr., A*, **2005**, 1074 (1–2), 71-
23 734 80.
- 24 735 41. H. O. T. Pye, R. W. Pinder, I. R. Piletic, Y. Xie, S. L. Capps, Y. -H. Lin, and E. O. Edney,
25 736 (2013). Epoxide pathways improve model predictions of isoprene markers and reveal key role
26 737 of acidity in aerosol formation, *Environ. Sci. Technol.*, **2013**, 47 (19), 11056-11064.
- 27 738 42. V. F. McNeill, Aqueous organic chemistry in the atmosphere: sources and chemical
28 739 processing of organic aerosols, *Environ. Sci. Technol.*, **2015**, 49 (3), 1237-1244.
- 29 740 43. E. A. Marais, D. J. Jacob, J. L. Jimenez, P. Campuzano-Jost, D. A. Day, W. Hu, J. Krechmer,
30 741 L. Zhu, P. S. Kim, C. C. Miller, J. A. Fisher, K. Travis, K. Yu, T. F. Hanisco, G. M. Wolfe, H.
31 742 L. Arkinson, H. O. T. Pye, K. D. Froyd, J. Liao and V. F. McNeill. Aqueous-phase
32 743 mechanism for secondary organic aerosol formation from isoprene: application to the
33 744 southeast United States and co-benefit of SO₂ emission controls, *Atmos. Chem. Phys.*, **2016**,
34 745 16 (3), 1603-1618.
- 35 746 44. A. L. Bondy, R. L. Craig, Z. Zhang, A. Gold, J. D. Surratt, and A. P. Ault, Isoprene-derived
36 747 organosulfates: vibrational mode analysis by Raman spectroscopy, acidity-dependent spectral
37 748 modes, and observation in individual atmospheric particles, *J. Phys. Chem. A*, **2018**, 122 (1),
38 749 303–315.
- 39 750 45. Z. Zhang, Y. -H. Lin, J. D. Surratt, L. M. Ball, and A. Gold, Technical Note: Synthesis of
40 751 isoprene atmospheric oxidation products: isomeric epoxydiols and the rearrangement products
41 752 *cis*- and *trans*-3-methyl-3,4-dihydroxytetrahydrofuran, *Atmos. Chem. Phys.*, **2012**, 12,
42 753 8529–8535.
- 43 754 46. A. Váradi, A. Gergely, S. Béni, P. Jankovics, B. Noszál, and S. Hosztafi, Sulfate esters of
44 755 morphine derivatives: Synthesis and characterization, *Eur J Pharm Sci.*, **2011**, 42 (1-2), 65-72.
- 45 756 47. H. Zhang, J. D. Surratt, Y. -H. Lin, J. Bapat, and R. M. Kamens, Effect of relative humidity
46 757 on SOA formation from isoprene/NO photooxidation: enhancement of 2-methylglyceric acid
47 758 and its corresponding oligoesters under dry conditions, *Atmos. Chem. Phys.*, **2011**, 11, 6411-
48 759 6424.

- 1
2
3 760 48. J. E. Krechmer, M. Groessl, X. Zhang, H. Junninen, P. Massoli, A. T. Lambe, J. R. Kimmel,
4 761 M. J. Cubison, S. Graf, Y.-H. Lin, S. H. Budisulistiorini, H. Zhang, J. D. Surratt, R.
5 762 Knochenmuss, J. T. Jayne, D. R. Worsnop, J. L. Jimenez, and M. R. Canagaratna, Ion
6 763 mobility spectrometry–mass spectrometry (IMS–MS) for on- and offline analysis of
7 764 atmospheric gas and aerosol species, *Atmos. Meas. Tech.*, **2016**, 9, 3245–3262.
- 8 765 49. T. B. Nguyen, K. H. Bates, J. D. Crouse, R. H. Schwantes, X. Zhang, H. G. Kjaergaard, J. D.
9 766 Surratt, P. Lin, A. Laskin, and J. H. Seinfeld, Mechanism of the hydroxyl radical oxidation of
10 767 methacryloyl peroxyxynitrate (MPAN) and its pathway toward secondary organic aerosol
11 768 formation in the atmosphere, *Phys. Chem. Chem. Phys.*, **2015**, 17 (27), 17914–17926.
- 12 769 50. S. S. de Sá, B. B. Palm, P. Campuzano-Jost, D. A. Day, M. K. Newburn, W. Hu, G.
13 770 Isaacman-VanWertz, L. D. Yee, R. Thalman, J. Brito, S. Carbone, P. Artaxo, A. H. Goldstein,
14 771 A. O. Manzi, R. A. F. Souza, F. Mei, J. E. Shilling, S. R. Springston, J. Wang, J. D. Surratt, M.
15 772 L. Alexander, J. L. Jimenez, and S. T. Martin, Influence of urban pollution on the production
16 773 of organic particulate matter from isoprene epoxydiols in central Amazonia, *Atmos. Chem.*
17 774 *Phys.*, **2017**, 17, 6611–6629.
- 18 775 51. A. Watanabe, S. J. Stropoli, and M. J. Elrod, Assessing the Potential Mechanisms of
19 776 Isomerization Reactions of Isoprene Epoxydiols on Secondary Organic Aerosol, *Environ. Sci.*
20 777 *Technol.* Just Accepted Manuscript, **2018**, DOI: 10.1021/acs.est.8b01780.
- 21 778 52. V. F. McNeill, J. L. Woo, D. D. Kim, A. N. Schwier, N. J. Wannell, A. J. Sumner, and J. M.
22 779 Barakat, Aqueous-phase secondary organic aerosol and organosulfate formation in
23 780 atmospheric aerosols: a modeling study, *Environ. Sci. Technol.*, **2012**, 46 (15), 8075–8081.
- 24 781 53. J. L. Woo and V. F. McNeill, SimpleGAMMA v1.0 – a reduced model of secondary organic
25 782 aerosol formation in the aqueous aerosol phase (aaSOA), *Geosci. Model Dev.*, **2015**, 8, 1821-
26 783 1829.
- 27 784 54. H. O. T. Pye, D. J. Luecken, L. Xu, C. M. Boyd, N. L. Ng, K. R. Baker, B. R. Ayres, J. O.
28 785 Bash, K. Baumann, W. P. L. Carter, E. Edgerton, J. L. Fry, W. T. Hutzell, D. B. Schwede, and
29 786 P. B. Shepson, Modeling the current and future roles of particulate organic nitrates in the
30 787 Southeastern United States, *Environ. Sci. Technol.*, **2015**, 49 (24), 14195–14203.
31 788

789 **Tables and Figures**

790

791 **Table 1.** Properties of the 2-methyltetrol, 2-methyltetrol sulfate and 3-methyltetrol sulfate standards characterized by HILIC/ESI-HR-
 792 Q-TOFMS, including retention times (RTs), linear range (L. Range), coefficient of determination (R^2), limit of detection (LOD), limit
 793 of quantification (LOQ) of ten replicate injections. Note that structures are for one of two diastereomers for each standard and ions are
 794 shown for the methyltetrol sulfates.

Standard	Synthesized Structural Isomer	Structure	[M-H] ⁻	<i>m/z</i>	RT(s) (min)	L. Range ($\mu\text{g mL}^{-1}$)	R^2	LOD ($\mu\text{g L}^{-1}$)	LOQ ($\mu\text{g L}^{-1}$)
2-methyltetrols	2-methylerythritol and 2-methylthreitol		$\text{C}_5\text{H}_{11}\text{O}_4^-$	135.066	4.0	0.01-25	0.9994	7.74	25.8
2-methyltetrol sulfates	1,3,4-trihydroxy-2-methylbutan-2-yl sulfate		$\text{C}_5\text{H}_{11}\text{O}_7\text{S}^-$	215.023	2.1, 2.6, 4.2, 5.2	0.01-10	0.9996	1.72	5.75
3-methyltetrol sulfates	2,3,4-trihydroxy-3-methylbutyl sulfate		$\text{C}_5\text{H}_{11}\text{O}_7\text{S}^-$	215.023	2.1, 2.6, 4.2, 5.2, 8.0, 8.3	0.01-25	1.0000	3.83	12.8

795

Table 2. Concentrations and mass fractions of 2-methyltetrols and methyltetrol sulfates measured from laboratory-generated SOA and ambient PM_{2.5} samples by HILIC/ESI-HR-QTOFMS.

	2-Methyltetrols		Methyltetrol sulfates	
	Mass Conc. (μg m ⁻³) ^a	% Total Mass ^b	Mass Conc. (μg m ⁻³)	% Total Mass
Laboratory β-IEPOX SOA	63.98	33.9 %	109.67	58.2 %
Laboratory δ-IEPOX SOA	29.49	19.6 %	62.98	41.9 %
Look Rock, TN, USA	0.861	5.6 (7.5) %	2.334	15.3 (12.9) %
Manaus, Brazil	0.137	(0.74) %	0.390	(1.34) %

^a The mass concentrations of 2-methyltetrols and methyltetrol sulfates were measured from the PILS samples for the laboratory-generated SOA, and from the filter samples for the Look Rock and Manaus samples;

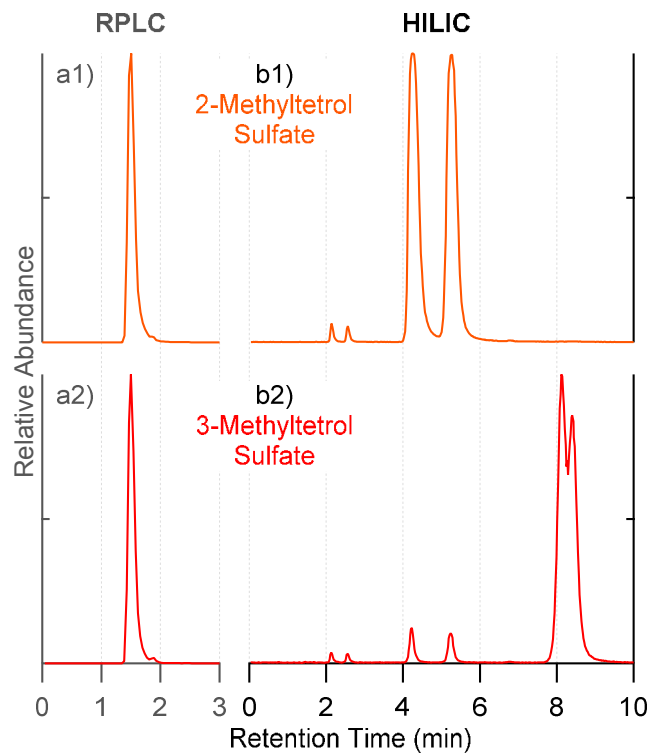
^b The total aerosol mass (organic + inorganic, shown in **bold**) was used for the mass closure for the laboratory-generated SOA, while the organic aerosol (or organic carbon, shown in parentheses) mass was used for the mass closure for the Look Rock and Manaus samples. The total aerosol mass was determined using an SEMS-MCPC system for the laboratory-generated SOAs, assuming the particle density to be 1.42 or 1.55 g cm⁻³ after reaction from β- or δ-IEPOX (SI). The total organic aerosol mass for the Look Rock sample was measured by an ACSM.^{11,12} The OC mass for the Look Rock and Manaus samples was measured using EC/OC analyzers. The relative analytical uncertainty in the quantification was determined to be up to ~14.1% (SI).

1
2
3 **812 Table 3.** Concentrations and discrepancies of 2-methyltetrols ($\mu\text{g m}^{-3}$) from laboratory-generated
4 **813** SOA and ambient $\text{PM}_{2.5}$ samples measured by HILIC/ESI-QTOFMS and GC/EI-MS.
5
6 **814**

2-Methyltetrols ($\mu\text{g m}^{-3}$)	HILIC/ESI- QTOFMS	GC/MS	Ratio (GC/HILIC)
Laboratory β -IEPOX SOA	69.05	140.86	204 %
Laboratory δ -IEPOX SOA	51.91	122.56	236 %
Look Rock, TN, USA	0.861	1.381	160 %
Manaus, Brazil	0.137	0.394	288 %

15 **815**

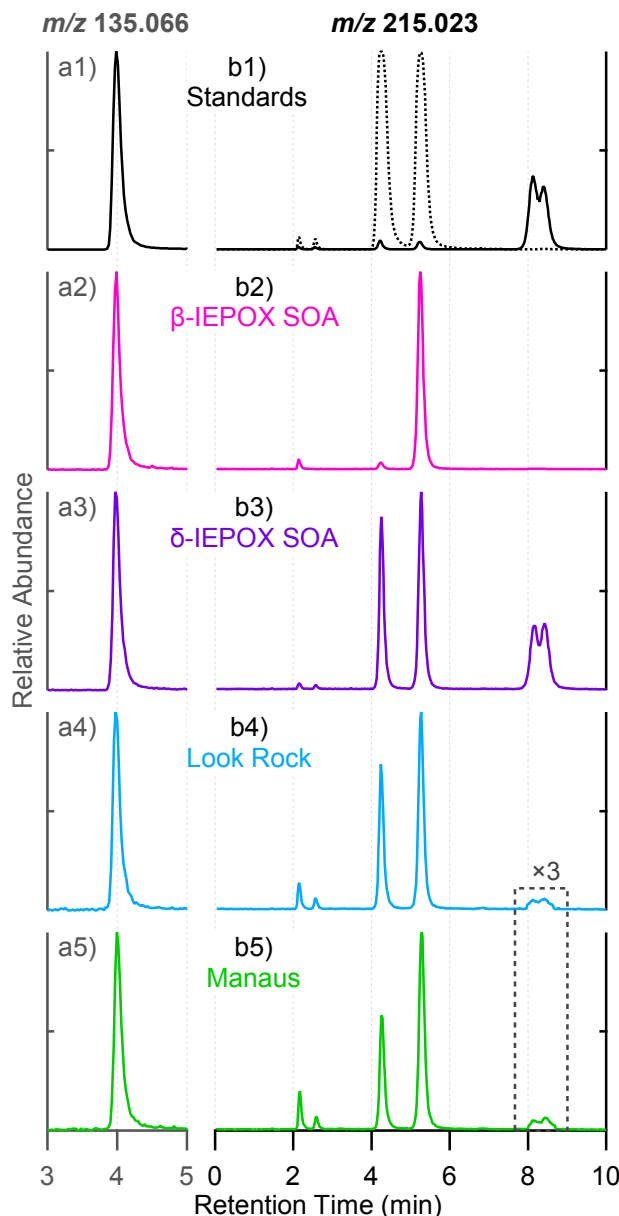
16
17 **816**
18
19
20
21
22
23
24
25
26
27
28
29
30
31
32
33
34
35
36
37
38
39
40
41
42
43
44
45
46
47
48
49
50
51
52
53
54
55
56
57
58
59
60



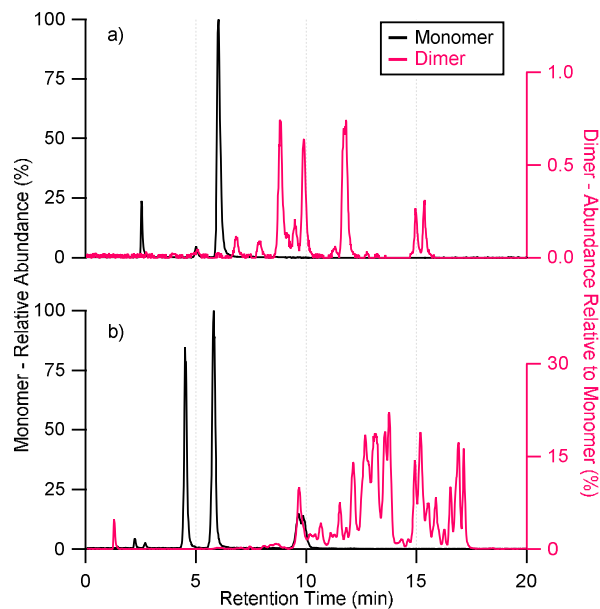
817

818 **Figure 1.** Extracted ion chromatograms (EICs) at m/z 215.023 corresponding to methyltetrol
819 sulfates. Using **a)** RPLC C_{18} column, and **b)** HILIC BEH amide column: standards of 1) 2-
820 methyltetrol sulfates; 2) 3-methyltetrol sulfates. Standards were prepared at $10 \mu\text{g mL}^{-1}$. No
821 significant peaks were observed beyond the shown periods of retention time.

822



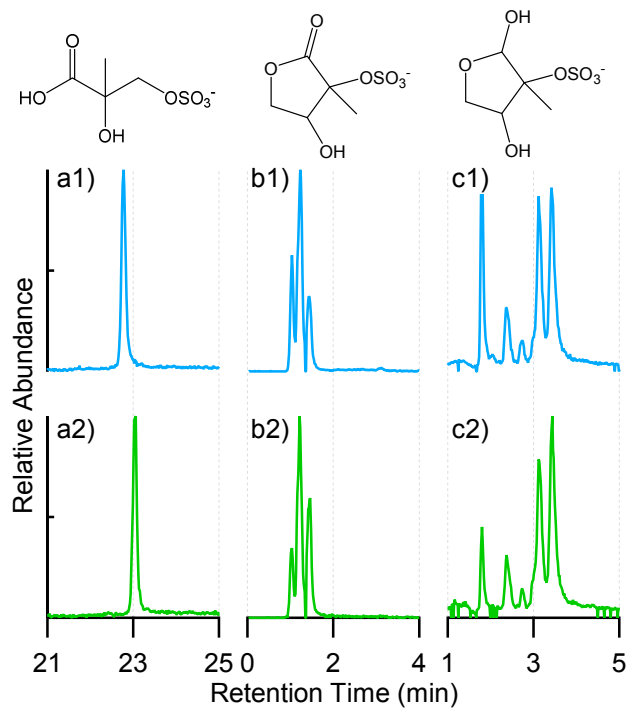
823
 824 **Figure 2.** EICs obtained from HILIC for **a)** m/z 135.066 corresponding to 2-methyltetrols, **b)** m/z
 825 215.023 corresponding to methyltetrol sulfates from: 1) $10 \mu\text{g mL}^{-1}$ synthesized standard (b1: 2-
 826 methyltetrol sulfates (dashed line) and 3-methyltetrol sulfates (solid line)); 2) laboratory-
 827 generated β -IEPOX SOA; 3) laboratory-generated δ -IEPOX SOA; 4) $\text{PM}_{2.5}$ sample collected at
 828 Look Rock during 2013 SOAS campaign; 5) $\text{PM}_{2.5}$ sample collected at Manaus in Nov. 2016.
 829 The laboratory-generated β -IEPOX SOA, δ -IEPOX SOA, Look Rock, and Manaus samples were
 830 diluted by a factor of 200, 100, 40, and 100, respectively. No significant peaks were observed
 831 beyond the shown periods of retention time.



832

833 **Figure 3.** EICs of m/z 215.023 ($C_5H_{11}O_7S^-$) and 333.086 ($C_{10}H_{21}O_{10}S^-$) corresponding to
834 methyltetrol sulfate monomers and dimers, respectively, from **a)** laboratory-generated β -IEPOX
835 SOA diluted by a factor of 200; and **b)** laboratory-generated δ -IEPOX SOA. No significant
836 peaks were observed beyond 20 min.

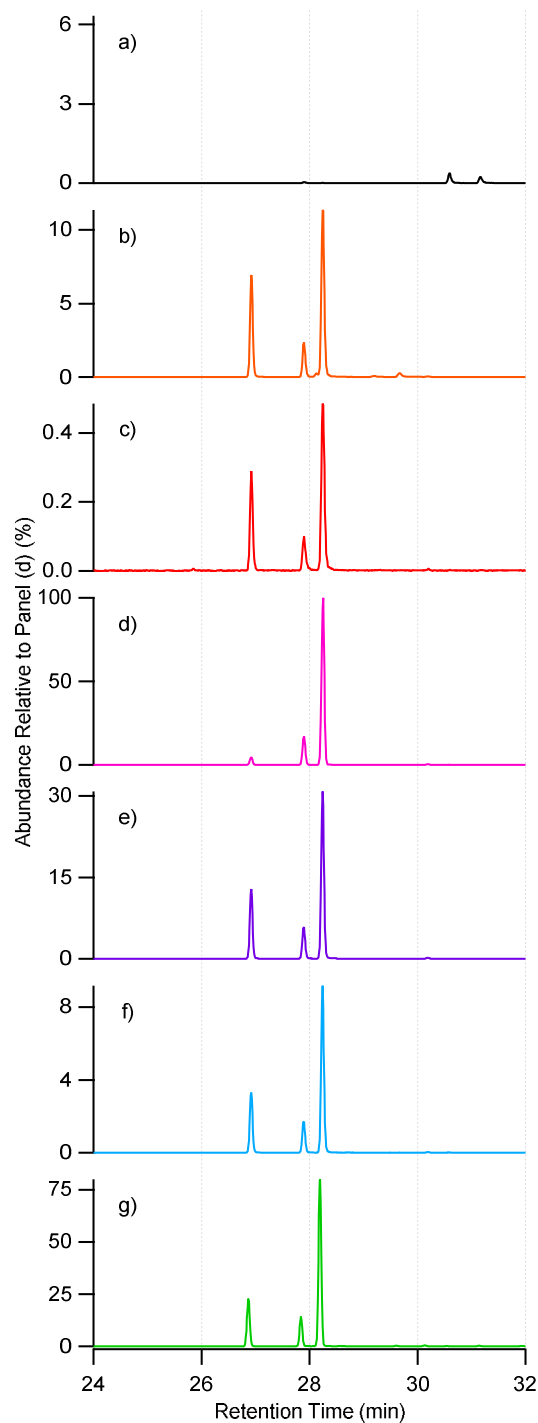
837



838

839 **Figure 4.** EICs of other water-soluble organosulfates with their proposed structures: **a)** m/z 199
840 corresponding to $C_4H_7O_7S^-$, **b)** m/z 211 corresponding to $C_5H_7O_7S^-$, and **c)** m/z 213
841 corresponding to $C_5H_9O_7S^-$ observed in $PM_{2.5}$ samples collected from 1) Look Rock during 2013
842 SOAS campaign; 2) Manaus in Nov. 2016. No significant peaks were observed beyond the
843 shown periods of retention time.

844



845
 846 **Figure 5.** GC/EI-MS EICs of m/z 231 corresponding to C_5 -alkene triols (RT = 26.9, 27.9, 28.3
 847 min) from: **a)** $50 \mu\text{g mL}^{-1}$ standard of 2-methyltetrol; **b)** $50 \mu\text{g mL}^{-1}$ standard of 2-methyltetrol
 848 sulfate; **c)** $50 \mu\text{g mL}^{-1}$ standard of 3-methyltetrol sulfate; **d)** laboratory-generated β -IEPOX SOA;
 849 **e)** laboratory-generated δ -IEPOX SOA; **f)** $\text{PM}_{2.5}$ sample at Look Rock during 2013 SOAS
 850 campaign; **g)** $\text{PM}_{2.5}$ sample at Manaus in Nov. 2016. Note that the y-axis scale was adjusted to
 851 the highest peak in each panel, with the labelled abundance in percentage relative to that in Panel
 852 (d).

1
2
3
4
5
6
7
8
9
10
11
12
13
14
15
16
17
18
19
20
21
22
23
24
25
26
27
28
29
30
31
32
33
34
35
36
37
38
39
40
41
42
43
44
45
46
47
48
49
50
51
52
53
54
55
56
57
58
59
60

853

41

Table of Contents Entry

One sentence of text, maximum 20 words, highlighting the novelty of the work:

A non-thermal analytical method is developed that can effectively resolve and quantify major IEPOX-derived SOA components in fine aerosol samples.

Graphic - maximum size 8 cm x 4 cm:

